*J. Fluid Mech.* (2009), *vol.* 637, *pp.* 327–356.  
doi:10.1017/S0022112009008052

# The equatorial counterpart of the quasi-geostrophic model

JÜRGEN THEISS[1]† AND ALI R. MOHEBALHOJEH[2]

[1]Theiss Research, PO Box 127, La Jolla, CA 92038, USA
[2]Institute of Geophysics, University of Tehran, PO Box 14155-6466, Tehran 14359, Iran

(Received 22 September 2008; revised 10 May 2009; accepted 13 May 2009; first published online 29 September 2009)

A uniformly valid balanced model that represents the quasi-geostrophic model's counterpart in the equatorial region is derived. The quasi-geostrophic model itself fails in the equatorial region because it is only valid where the dominant balance is geostrophic, i.e. where the Rossby number is small. The smallness of the Rossby number is assumed in the quasi-geostrophic model's standard derivation and therefore this derivation cannot be repeated for the equatorial region. An alternative derivation of the quasi-geostrophic model that is independent of the Rossby number was presented by Leith in 1980, using the geometric framework of nonlinear normal mode initialization. Its independence of the Rossby number allows it to be repeated for the equatorial region, leading to an equatorial balanced model that thus represents the equatorial counterpart of the quasi-geostrophic model. As such it also coincides with the quasi-geostrophic model sufficiently far away from the equator. Its dispersion relation can be expressed in an explicit analytic form and, compared to that of other balanced models of similar simplicity, approximates that of the shallow water equations strikingly well.

## 1. Introduction

A large variety of atmospheric and oceanic flows, ranging from mesoscale eddies to the general circulation, is dominantly balanced flows and can therefore be described by balanced models. These balanced models facilitate theoretical and numerical studies because by construction they describe only the low-frequency dynamics represented by Rossby waves whereas the primitive equations, i.e. the full equations of motion, also describe the high-frequency dynamics represented by inertia–gravity waves. The most prominent of such balanced models is the quasi-geostrophic model (e.g. Salmon 1998; Vallis 2006).

In the case of a shallow layer of fluid with constant density considered in this paper, the primitive equations become the shallow water equations. They consist of the three evolution equations of the horizontal velocity components and the height. By contrast, a balanced model derived from the shallow water equations consists of only one evolution equation and two balance relations. In the case of the quasi-geostrophic model, they are the evolution equation of linear potential vorticity and two geostrophic balance relations expressing geostrophy. The derivation thus reduces the number of evolution equations from three to one, which reflects the fact that the quasi-geostrophic model, like any other balanced model, has only one low-frequency

† Email address for correspondence: j.theiss@theissresearch.org

normal mode represented by Rossby waves, whereas the shallow water equations have in addition two high-frequency normal modes represented by inertia–gravity waves.

In the majority of cases the dynamics is characterized by either the Rossby or Froude number or both being small as well as a separation between the frequencies of Rossby and inertia–gravity waves. These two characteristics allow balanced models to be asymptotic approximations of the primitive equations. An example is the quasi-geostrophic model, valid outside the equatorial region, where the Rossby number is small and the frequencies separated. The dynamics in the equatorial region, unfortunately, lacks these two characteristics because the Rossby number is large and tends to infinity at the equator and the frequencies are not clearly separated, due to the equatorial Kelvin wave (e.g. Bokhove 1997) and the mixed Rossby–gravity wave, also referred to as the Yanai wave. However, the concept of balance remains robust well beyond cases of flows that can be described by asymptotic approximations (e.g. Tribbia 1979; McIntyre & Norton 2000) and therefore balanced models for the equatorial region are generally possible.

There are already balanced models in the literature that are valid in the equatorial region. A group of such models share a simple construction. In the case of the shallow water equations, they are constructed by re-writing the shallow water equations as three evolution equations of potential vorticity, or some approximation to it, velocity divergence and acceleration divergence. For the balanced model, the evolution equation is taken to be that of potential vorticity and the two balance relations obtained by setting to zero two time derivatives of suitably chosen orders of the two other variables, i.e. velocity divergence and acceleration divergence (e.g. Mohebalhojeh & Dritschel 2001; Mohebalhoje & McIntyre 2007*a*,*b*). A well-known balanced model with a similar construction is the Bolin–Charney model (Bolin 1955; Charney 1955, 1962), often referred to as the Balance Equations, where a nonlinear redefinition of acceleration divergence and its time derivative are used to define the two balance relations (Mohebalhoje & McIntyre 2007*a*,*b*).

Undoubtedly, the most prominent balanced model is the quasi-geostrophic model, but it is not valid in the equatorial region. This motivates the derivation of its counterpart in the equatorial region, presented in this paper and referred to as the equatorial balanced model. It differs from the existing balanced models and compared to them approximates more accurately the dispersion relation of the shallow water equations. To derive it we cannot repeat the standard derivation of the quasi-geostrophic model for the equatorial region because it requires the Rossby number to be small, which is not the case. Physically, this means that in the equatorial region the dominant balance is not simply between two forces, as it is the case outside it, where it defines geostrophic balance and thus implies a small Rossby number. We therefore choose instead to repeat for the equatorial region the alternative derivation of the quasi-geostrophic model within a geometric framework given by Leith (1980) because it is independent of Rossby number.

Leith's derivation uses the phase space in which every possible state of a fluid is uniquely represented by a single point. In the case of the shallow water equations, the state of the fluid is given by the two horizontal velocity components and the height perturbation at every horizontal location. At each horizontal location it can therefore be uniquely represented by a single point in a three-dimensional space. If the three variables are Fourier transformed then there is a three-dimensional space not for every horizontal location but rather for every horizontal wavenumber. Combining all such mutually orthogonal three-dimensional spaces comprise the phase space. Each of the three-dimensional spaces is spanned by three orthonormal vectors and these are taken to be the eigenvectors of the linearized shallow water equations. The corresponding eigenvalues, which are the characteristic frequencies, allow the eigenvectors to be distinguished between those of the one low-frequency or Rossby normal mode, represented by Rossby waves, and the two high-frequency or gravity normal modes, represented by inertia–gravity waves. Thus, each state of the fluid can be decomposed into a high- and a low-frequency component by projecting the corresponding single point in phase space onto the mutually orthogonal Rossby and gravity manifolds, or subspaces, spanned by the eigenvectors associated with the Rossby and gravity normal modes, respectively. The Rossby and gravity normal modes and manifolds are in Leith (1980) called rotational and gravitational, respectively.

In the special case of linear dynamics, the balanced dynamics is described by the linearized primitive equations, which in our case are the linearized shallow water equations, with an initial state of the fluid represented by a single point on the Rossby manifold. This single point would then always remain on the Rossby manifold during the evolution, thus corresponding to low-frequency, i.e. balanced, dynamics.

In the general case of nonlinear dynamics, the single point initially on the Rossby manifold would move off it. This would create a projection onto the gravity manifold and thus the dynamics would contain an unwanted high-frequency component. Balanced states with minimal excitation of high-frequency components nevertheless exist and are represented by points on the slow manifold (Leith 1980) in phase space. Similarly to the linear case, for which the single point representing the dynamics remains on the Rossby manifold, in the nonlinear case the single point remains on the slow manifold. This is a practical view although the slow manifold in its strict sense does not exist and is rather a thin stochastic layer (Ford, McIntyre & Norton 2000), which however is not of concern in this paper. Finding the slow manifold by an iterative method has been a central goal of nonlinear normal mode initialization (Baer 1977; Baer & Tribbia 1977; Machenhauer 1977). The first iterative step gives an approximation to the slow manifold. Leith (1980) made the remarkable discovery that for the case of a mid-latitude $f$-plane the evolution of a single point on this approximate slow manifold projected onto the Rossby manifold is described by the quasi-geostrophic model. This alternative derivation of the quasi-geostrophic model is independent of Rossby number and generally not restricted to the outside of the equatorial region. We therefore repeat it for the case of an equatorial $\beta$-plane and thus derive the equatorial counterpart of the quasi-geostrophic model, referred to as the equatorial balanced model.

The quasi-geostrophic model has been widely used to study strongly nonlinear dynamics in the mid-latitudes, also known as geostrophic turbulence, featuring processes such as energy cascades and the formation and maintenance of zonal flows. Theiss (2004) showed, using the quasi-geostrophic model, that these phenomena change with decreasing latitude. This has motivated us to derive the equatorial balanced model as it allows the study of these phenomena to be extended to the equatorial region, where the quasi-geostrophic model is invalid.

In the following section, we review the geometric framework used by Leith (1980) in more specific terms. The shallow water equations are introduced in § 3 and we present in § 4 the derivation of the quasi-geostrophic model on a mid-latitude $f$-plane within this geometric framework by analogy to Leith (1980). This then serves in § 5 as guidance to repeat the derivation on an equatorial $\beta$-plane, giving the equatorial balanced model that is thus the equatorial counterpart of the quasi-geostrophic model. Limits in which the equatorial balanced model takes simpler forms are investigated in § 6, extensions needed to describe also bounded, forced and stratified fluids are given in §7, comparisons of the equatorial balanced model to other balanced models of comparable simplicity are made in §8. Section 9 summarizes the equatorial balanced model and its properties.

## 2. Geometric framework

Every possible state of a fluid can be represented by a single point in phase space, as described in the previous section. This single point at a particular time $t$ is expressed by the vector $\boldsymbol{x}^s(t)$. In our case of the dynamics of a shallow layer of fluid with constant density described by the shallow water equations, the vector takes on the form $\boldsymbol{x}^s(t) = [\boldsymbol{u}(\cdot, t), \eta(\cdot, t)]$, where $\boldsymbol{u} = (u, v)$ is the horizontal velocity vector with $u$ and $v$ being its components in the $x$, or zonal, direction and $y$, or meridional, direction, respectively, $\eta$ the scaled height perturbation, and the dots represent the dependence on the horizontal location either in physical, wavenumber or physical–wavenumber space.

In terms of the vector $\boldsymbol{x}^s$, the primitive equations, which in our case are the shallow water equations, take the general form

$$\dot{\boldsymbol{x}}^s = -\mathrm{i}\mathscr{L}\boldsymbol{x}^s + \mathscr{N}(\boldsymbol{x}^s), \tag{2.1}$$

where the dot represents the partial time derivative, $\mathscr{L}$ is a linear Hermitian operator, $\mathscr{N}$ a nonlinear vector function and i the imaginary unit. Because $\mathscr{L}$ is Hermitian its eigenvectors are a complete orthogonal set (e.g. Wilkinson 1988, p. 25) and therefore they are taken to span the phase space. They can be partitioned into sets of three eigenvectors, where each set corresponds to a particular horizontal location in either physical, wavenumber or physical–wavenumber space. The eigenvectors respectively corresponding to the smallest eigenvalue in a set are those of the one low-frequency Rossby normal mode and span the Rossby manifold. The remaining eigenvectors are those of the two high-frequency gravity normal modes and span the gravity manifold. The phase space is therefore spanned by the mutually orthogonal Rossby and gravity manifolds.

The slow manifold in phase space, as described in the previous section, is defined by Machenhauer (1977) by $\mathscr{G}\dot{\boldsymbol{x}}^s = 0$, where $\mathscr{G}$ is an operator projecting a point in phase space onto the gravity manifold. In the special case of linear dynamics, applying this definition to (2.1) and using the fact that in this case $\mathscr{N} = 0$, gives the condition $\mathscr{G}\mathscr{L}\boldsymbol{x}^s = 0$. The operators $\mathscr{G}$ and $\mathscr{L}$ commute, i.e. $\mathscr{G}\mathscr{L} = \mathscr{L}\mathscr{G}$, because they share the same set of eigenvectors (e.g. Wilkinson 1988, p. 52). Furthermore, any vector in the gravity manifold can be decomposed into a linear combination of eigenvectors of $\mathscr{L}$. Using these two properties, allows the condition to be written as $\mathscr{G}\boldsymbol{x}^s = 0$. This implies that $\boldsymbol{x}^s$ must lie on the Rossby manifold and therefore in the special case of linear dynamics, the slow manifold is the Rossby manifold. For the general case of nonlinear dynamics, we repeat the steps discussed above but with $\mathscr{N} \neq 0$ and use the trivial identity $\mathscr{G} = \mathscr{G}\mathscr{G}$. The condition describing the slow manifold then becomes

$$\mathscr{G}\boldsymbol{x}^s = -\mathrm{i}\,(\mathscr{L}\mathscr{G})^{-1}\,\mathscr{G}\mathscr{N}(\boldsymbol{x}^s). \tag{2.2}$$

This implies that the slow manifold is distinct from the Rossby manifold. The slow manifold therefore has a non-zero projection onto the gravity manifold, which is inconsistent with its definition, given by $\mathscr{G}\dot{\boldsymbol{x}}^s = 0$. Although this could be corrected (Baer 1977), we do not make the correction because it has no effect on the first step of the iteration below, which is the only step of concern in this paper.

Condition (2.2) is solved iteratively. As the first step, a vector in the Rossby manifold, denoted by $\boldsymbol{x}^s = \boldsymbol{y}_0^s$, is inserted on the right-hand side of (2.2), resulting in $\boldsymbol{x}^s = \boldsymbol{z}_1^s$ on the left-hand side, where $\boldsymbol{z}_1^s$ denotes a vector in the gravity manifold. This can be generalized to $\boldsymbol{x}^s = \boldsymbol{y}_0^s + \boldsymbol{z}_1^s$ because of $\mathscr{G}\boldsymbol{y}_0^s = 0$. This first iterative step therefore defines a function of the form $\boldsymbol{z}_1^s(\boldsymbol{y}_0^s)$, which describes an approximate slow manifold. As the second step, $\boldsymbol{x}^s = \boldsymbol{y}_0^s + \boldsymbol{z}_1^s$ is inserted on the right-hand side, resulting in $\boldsymbol{x}^s = \boldsymbol{y}_0^s + \boldsymbol{z}_2^s$ on the left-hand side and so on until the iteration converges and thus the slow manifold is obtained.

The approximate slow manifold obtained by the first iterative step is identical to that obtained by the Baer–Tribbia initialization scheme (Baer & Tribbia 1977) to first order, which is given by (2.6*a*) in Tribbia (1979). This becomes apparent by establishing the one-to-one correspondence between Tribbia's and our notation, which is $\xi = \boldsymbol{x}^s$, $\boldsymbol{y} = \mathscr{G}\boldsymbol{x}^s$, $\Lambda_y \boldsymbol{y} = -\mathrm{i}\mathscr{L}\mathscr{G}\boldsymbol{x}^s$, $\epsilon G_y(\xi, \xi) = \mathscr{G}\mathscr{N}(\boldsymbol{x}^s)$ and $\xi_0 = \boldsymbol{y}_0^s$. The Baer–Tribbia initialization scheme, unlike the scheme based on Machenhauer (1977) adopted above, requires a frequency separation. Tribbia (1979), however, shows that for the case of an equatorial $\beta$-plane, on which there is no complete frequency separation, it nevertheless performs well. This thus demonstrates for the equatorial balanced model derived in this paper the general understanding, noted in § 1, that the concept of balance remains robust even in cases that lack a frequency separation.

The evolution of a single point on the above approximate slow manifold represents an approximate balanced dynamics. In order to obtain an equation describing this evolution, we take the definition of the approximate slow manifold, i.e. inserting as above $\boldsymbol{x}^s = \boldsymbol{y}_0^s$ on the right-hand side and $\boldsymbol{x}^s = \boldsymbol{y}_0^s + \boldsymbol{z}_1^s$ on the left-hand side of (2.2). Retracing the steps from (2.2) to (2.1) then gives

$$\dot{\boldsymbol{x}}^s = -\mathrm{i}\mathscr{L}\boldsymbol{x}^s + \mathscr{N}(\boldsymbol{y}_0^s), \tag{2.3}$$

where in this case $\boldsymbol{x}^s = \boldsymbol{y}_0^s + \boldsymbol{z}_1^s$. Leith (1980) points out that rather than considering the evolution on the approximate slow manifold described by (2.3), its projection onto the Rossby manifold can be considered. The evolution on the approximate slow manifold is then determined diagnostically, using the definition of the approximate slow manifold, given by $\boldsymbol{z}_1^s(\boldsymbol{y}_0^s)$. The required projection operator is denoted by $\mathscr{R}$. It commutes with $\mathscr{L}$ for the same reason $\mathscr{G}$ commutes with $\mathscr{L}$, explained above, as well as with the partial time derivative. The evolution described by (2.3) projected onto the Rossby manifold, using $\mathscr{R}\boldsymbol{x}^s = \boldsymbol{y}_0^s$, is therefore given by

$$\dot{\boldsymbol{y}}_0^s = -\mathrm{i}\mathscr{L}\boldsymbol{y}_0^s + \mathscr{R}\mathscr{N}(\boldsymbol{y}_0^s). \tag{2.4}$$

Leith (1980) shows that (2.4) on a mid-latitude $f$-plane is identical to the quasi-geostrophic model. This fundamental insight inspires us to consider (2.4) on an equatorial $\beta$-plane, which gives an equatorial balanced model that thus is the equatorial counterpart of the quasi-geostrophic model.

## 3. Shallow water equations

The primitive equations are in this paper always those describing the dynamics of a shallow layer of fluid with constant density. They are therefore the shallow water equations, given by

$$\frac{\mathrm{D}\boldsymbol{u}}{\mathrm{D}t} + f\hat{\boldsymbol{k}} \times \boldsymbol{u} = -g\nabla h \tag{3.1}$$

$$\frac{\partial h}{\partial t} + \nabla \cdot (h\boldsymbol{u}) = 0, \tag{3.2}$$

where the horizontal velocity vector $\boldsymbol{u}$ and the height $h$ depend in this case on $(\boldsymbol{x}, t)$ with $\boldsymbol{x} = (x, y)$ being the horizontal location in physical space. Furthermore, we have $\mathrm{D}/\mathrm{D}t = \partial/\partial t + \boldsymbol{u} \cdot \nabla$, $f$ the Coriolis parameter, $\hat{\boldsymbol{k}}$ the vertical unit vector, $g$ the acceleration due to gravity and $\nabla = (\partial/\partial x, \partial/\partial y)$. The height is expressed as $h = H + \sqrt{H/g}\,\eta$, where $H$ is the layer depth at rest and $\sqrt{H/g}\,\eta$ the height perturbation. The scaling of the height perturbation gives $\eta$ the dimension of velocity. In terms of $\eta$, (3.1) and (3.2) become

$$\frac{\mathrm{D}\boldsymbol{u}}{\mathrm{D}t} + f\hat{\boldsymbol{k}} \times \boldsymbol{u} = -c\nabla\eta \tag{3.3}$$

$$\frac{\partial \eta}{\partial t} + \nabla \cdot [(c+\eta)\boldsymbol{u}] = 0, \tag{3.4}$$

where $c = \sqrt{gH}$. In the geometric framework, introduced in the previous section, the shallow water equations (3.3) and (3.4) have the general form (2.1), where

$$\mathscr{L} = \begin{pmatrix} 0 & \mathrm{i}f & -\mathrm{i}c\frac{\partial}{\partial x} \\ -\mathrm{i}f & 0 & -\mathrm{i}c\frac{\partial}{\partial y} \\ -\mathrm{i}c\frac{\partial}{\partial x} & -\mathrm{i}c\frac{\partial}{\partial y} & 0 \end{pmatrix}, \quad \mathscr{N} = \begin{pmatrix} -\boldsymbol{u}\cdot\nabla u \\ -\boldsymbol{u}\cdot\nabla v \\ -\nabla\cdot(\eta\boldsymbol{u}) \end{pmatrix}, \quad \boldsymbol{x}^s = \begin{pmatrix} u(\boldsymbol{x}, t) \\ v(\boldsymbol{x}, t) \\ \eta(\boldsymbol{x}, t) \end{pmatrix}. \tag{3.5}$$

The linear operator $\mathscr{L}$ is Hermitian (appendix A). This implies that its eigenvalues, which are the characteristic frequencies of the shallow layer of fluid with constant density, are real and that its eigenvectors are a complete set of orthogonal vectors (e.g. Wilkinson 1988, p. 25), which are therefore taken to span the phase space. To determine the eigenvalues and eigenvectors, we solve

$$(\mathscr{L} - \omega\mathbf{I})\,\boldsymbol{x}^s = 0, \tag{3.6}$$

where $\mathbf{I}$ is the identity matrix and $\omega$ an eigenvalue, satisfying $\det(\mathscr{L} - \omega\mathbf{I}) = 0$. We re-write (3.6) by first expressing $\boldsymbol{x}^s$ in terms of its Fourier transform in the $x$-direction, which takes the form

$$[\boldsymbol{u}(\boldsymbol{x}, t), \eta(\boldsymbol{x}, t)] = \frac{1}{\sqrt{2\pi}} \int_{-\infty}^{\infty} [\tilde{\boldsymbol{u}}(k', y, t), \tilde{\eta}(k', y, t)] \mathrm{e}^{\mathrm{i}k'x}\, \mathrm{d}k'. \tag{3.7}$$

We then multiply by $\exp(-\mathrm{i}kx)/\sqrt{2\pi}$ and integrate over all $x$, which gives

$$(\mathscr{L} - \omega\mathbf{I})\,\boldsymbol{x}^s = \begin{pmatrix} -\omega & \mathrm{i}f & ck \\ -\mathrm{i}f & -\omega & -\mathrm{i}c\frac{\partial}{\partial y} \\ ck & -\mathrm{i}c\frac{\partial}{\partial y} & -\omega \end{pmatrix} \begin{pmatrix} \tilde{u}(k, y, t) \\ \tilde{v}(k, y, t) \\ \tilde{\eta}(k, y, t) \end{pmatrix} = 0, \tag{3.8}$$

where $k$ is the wavenumber in the $x$-direction and the dependence of $\boldsymbol{x}^s$ changed from $(\boldsymbol{x}, t)$ to $(k, y, t)$. For the case $k \neq 0$, we use the row manipulations given in appendix B, thus re-writing (3.8) as

$$(\mathscr{L} - \omega I)\,\boldsymbol{x}^s = \begin{pmatrix} \left(\frac{\omega}{c}\right)^2 - k^2 & \mathrm{i}k\frac{\partial}{\partial y} - \mathrm{i}\frac{\omega}{c}\frac{f}{c} & 0 \\ 0 & \mathrm{i}\frac{\omega}{c}\frac{\partial}{\partial y} - \mathrm{i}\frac{f}{c}k & \left(\frac{\omega}{c}\right)^2 - k^2 \\ 0 & \omega\left[\left(\frac{\omega}{c}\right)^2 - k^2 + \frac{\partial^2}{\partial y^2} - \frac{f^2}{c^2}\right] - \frac{\partial f}{\partial y}k & 0 \end{pmatrix} \begin{pmatrix} \tilde{u}(k, y, t) \\ \tilde{v}(k, y, t) \\ \tilde{\eta}(k, y, t) \end{pmatrix} = 0. \tag{3.9}$$

This is used in the following sections to calculate the eigenvalues and eigenvectors for specific cases of $f$.

## 4. Quasi-geostrophic model

Leith (1980) uses the geometric framework to derive the quasi-geostrophic model. His approach is outlined in general terms in § 2 and in this section we present as a concrete example the derivation of the quasi-geostrophic model from the shallow water equations on an $f$-plane. This serves in particular as guidance for the derivation of the equatorial balanced model in the next section.

For an $f$-plane, $f = f_0$, where $f_0$ is a constant. To determine the eigenvalues and eigenvectors for this particular case we solve (3.8) for $k = 0$ and (3.9) for $k \neq 0$. We first express $\boldsymbol{x}^s$ in (3.8) and (3.9) in terms of its Fourier transform in the $y$-direction, which takes the form

$$[\tilde{\boldsymbol{u}}(k, y, t), \tilde{\eta}(k, y, t)] = \frac{1}{\sqrt{2\pi}} \int_{-\infty}^{\infty} [\hat{\boldsymbol{u}}(k, l', t), \hat{\eta}(k, l', t)] \mathrm{e}^{\mathrm{i}l'y} \, \mathrm{d}l'. \tag{4.1}$$

We then multiply by $\exp(-\mathrm{i}ly)/\sqrt{2\pi}$, and integrate over all $y$, which gives

$$\begin{pmatrix} -\omega & \mathrm{i}f_0 & 0 \\ -\mathrm{i}f_0 & -\omega & cl \\ 0 & cl & -\omega \end{pmatrix} \begin{pmatrix} \hat{u}(\boldsymbol{k}, t) \\ \hat{v}(\boldsymbol{k}, t) \\ \hat{\eta}(\boldsymbol{k}, t) \end{pmatrix} = 0 \tag{4.2}$$

and

$$\begin{pmatrix} \left(\frac{\omega}{c}\right)^2 - k^2 & -kl - \mathrm{i}\frac{\omega}{c}\frac{f_0}{c} & 0 \\ 0 & -\frac{\omega}{c}l - \mathrm{i}\frac{f_0}{c}k & \left(\frac{\omega}{c}\right)^2 - k^2 \\ 0 & \omega\left[\left(\frac{\omega}{c}\right)^2 - k^2 - l^2 - \frac{f_0^2}{c^2}\right] & 0 \end{pmatrix} \begin{pmatrix} \hat{u}(\boldsymbol{k}, t) \\ \hat{v}(\boldsymbol{k}, t) \\ \hat{\eta}(\boldsymbol{k}, t) \end{pmatrix} = 0, \tag{4.3}$$

for $k = 0$ and $k \neq 0$, respectively, where $l$ is the wavenumber in the $y$-direction and $\boldsymbol{k} = (k, l)$ the wavenumber vector. The eigenvalues for $k = 0$ have the same general form as those for $k \neq 0$, which are the solutions of the bottom centre matrix element in (4.3) set to zero and are given by

$$\omega_R = 0, \quad \omega_{G^+} = c\sigma, \quad \omega_{G^-} = -c\sigma, \tag{4.4}$$

where $\sigma = \sqrt{k^2 + l^2 + f_0^2/c^2}$. The corresponding eigenvectors also have the same general forms for $k = 0$ and $k \neq 0$ and are given by

$$\hat{\boldsymbol{e}}_R = \frac{1}{\sigma} \begin{pmatrix} -\mathrm{i}l \\ \mathrm{i}k \\ \frac{f_0}{c} \end{pmatrix}, \quad \hat{\boldsymbol{e}}_{G^+} = \frac{1}{\sqrt{2}|\boldsymbol{k}|\sigma} \begin{pmatrix} \sigma k + \mathrm{i}\frac{f_0}{c}l \\ \sigma l - \mathrm{i}\frac{f_0}{c}k \\ k^2 + l^2 \end{pmatrix}, \quad \hat{\boldsymbol{e}}_{G^-} = \frac{1}{\sqrt{2}|\boldsymbol{k}|\sigma} \begin{pmatrix} -\sigma k + \mathrm{i}\frac{f_0}{c}l \\ -\sigma l - \mathrm{i}\frac{f_0}{c}k \\ k^2 + l^2 \end{pmatrix}, \tag{4.5}$$

where the use of the hat on each eigenvector indicates that the eigenvectors are normalized and where $|\boldsymbol{k}| = \sqrt{k^2 + l^2}$. As stated in the previous section, the eigenvalues are real and the eigenvectors are a complete orthogonal set. The pair $\omega_R$ and $\hat{\boldsymbol{e}}_R$ represents the low-frequency Rossby normal mode and $\omega_{G\pm}$ and $\hat{\boldsymbol{e}}_{G\pm}$ the high-frequency gravity normal modes. The eigenvector $\hat{\boldsymbol{e}}_R$ spans the Rossby manifold on which a vector $\boldsymbol{y}_0^s$ is expressed as

$$\boldsymbol{y}_0^s = (\hat{\boldsymbol{u}}_R, \hat{\eta}_R) = \hat{\boldsymbol{e}}_R(\boldsymbol{k}) R(\boldsymbol{k}, t), \tag{4.6}$$

where $R(\boldsymbol{k}, t)$ is the coordinate of the vector $\boldsymbol{y}_0^s$ on the Rossby manifold.

To understand what the Rossby manifold represents physically, we Fourier transform (4.6), using first (4.1) and then (3.7), giving

$$\boldsymbol{y}_0^s = (\boldsymbol{u}_R, \eta_R) = \boldsymbol{e}_R(\boldsymbol{x})\psi(\boldsymbol{x}, t), \tag{4.7}$$

where $\boldsymbol{e}_R(\boldsymbol{x})$ is not normalized and given by

$$\boldsymbol{e}_R(\boldsymbol{x}) = \begin{pmatrix} -\dfrac{\partial}{\partial y} \\ \dfrac{\partial}{\partial x} \\ \dfrac{f_0}{c} \end{pmatrix} \tag{4.8}$$

and

$$\psi(\boldsymbol{x}, t) = \frac{1}{2\pi} \int_{-\infty}^{\infty} \int_{-\infty}^{\infty} \frac{R(\boldsymbol{k}, t)}{\sigma} \mathrm{e}^{\mathrm{i}\boldsymbol{k}\cdot\boldsymbol{x}}\, \mathrm{d}\boldsymbol{k}. \tag{4.9}$$

Re-writing (4.7) by eliminating $\psi(\boldsymbol{x}, t)$, results in

$$f_0 \hat{\boldsymbol{k}} \times \boldsymbol{u}_R = -c\nabla\eta_R, \tag{4.10}$$

which is the geostrophic balance relation. A vector $\boldsymbol{y}_0^s$ on the Rossby manifold therefore represents a state of the fluid that is in geostrophic balance.

In §2 it is stated that for the present case of an $f$-plane, (2.4) is identical to the quasi-geostrophic model. To verify this, we specify $\mathscr{R} = \hat{\boldsymbol{e}}_R \cdot \hat{\boldsymbol{e}}_R^{\dagger}$, where '†' denotes the conjugate transpose, or adjoint, defined in appendix A, and multiply (2.4) from the left by $\boldsymbol{e}_R^{\dagger}$, where $\boldsymbol{e}_R$ is not normalized. Because $\hat{\boldsymbol{e}}_R^{\dagger} \cdot \hat{\boldsymbol{e}}_R = 1$, we thus obtain

$$\boldsymbol{e}_R^{\dagger} \cdot \dot{\boldsymbol{y}}_0^s = -\mathrm{i}\boldsymbol{e}_R^{\dagger} \cdot \mathscr{L}\boldsymbol{y}_0^s + \boldsymbol{e}_R^{\dagger} \cdot \mathscr{N}(\boldsymbol{y}_0^s). \tag{4.11}$$

Because $\boldsymbol{e}_R^{\dagger} \cdot \boldsymbol{y}_0^s = \boldsymbol{e}_R^{\dagger} \cdot \boldsymbol{x}^s$ and $\boldsymbol{y}_0^s$ is an eigenvector of $\mathscr{L}$, this can be written as

$$\boldsymbol{e}_R^{\dagger} \cdot \dot{\boldsymbol{x}}^s = -\mathrm{i}\boldsymbol{e}_R^{\dagger} \cdot \mathscr{L}\boldsymbol{x}^s + \boldsymbol{e}_R^{\dagger} \cdot \mathscr{N}(\boldsymbol{y}_0^s), \tag{4.12}$$

which is identical to (2.3) multiplied from the left by $\boldsymbol{e}_R^{\dagger}$.

An explicit expression for the nonlinear term in (4.11) or (4.12) is obtained in a similar way as those above for the linear terms. We thus substitute (3.7) with (4.1) into $\mathscr{N}$ in (3.5), multiply by $\exp(-\mathrm{i}\boldsymbol{k}\cdot\boldsymbol{x})/2\pi$, integrate over all $\boldsymbol{x}$, and multiply the result from the left by $\boldsymbol{e}_R^{\dagger}$.

Because $\boldsymbol{y}_0^s$, given by (4.6), is an eigenvector of $\mathscr{L}$ with a zero eigenvalue, as shown in (4.4), the first term on the right-hand side of (4.11) vanishes and thus (4.11) becomes

$$\boldsymbol{e}_R^{\dagger} \cdot \dot{\boldsymbol{y}}_0^s = \boldsymbol{e}_R^{\dagger} \cdot \mathscr{N}(\boldsymbol{y}_0^s). \tag{4.13}$$

Substituting $\boldsymbol{y}_0^s$ given by the first equation in (4.6) into (4.13) and Fourier transforming as defined by (4.1) and (3.7), gives

$$\frac{\partial q}{\partial t} + \boldsymbol{u}_R \cdot \nabla q = 0, \tag{4.14}$$

where

$$q = \frac{\partial v_R}{\partial x} - \frac{\partial u_R}{\partial y} - \frac{f_0}{c}\eta_R. \tag{4.15}$$

By using (4.7), these can be re-written as

$$\frac{\partial q}{\partial t} + J(\psi, q) = 0, \tag{4.16}$$

where $J(\psi, q) = \partial\psi/\partial x\ \partial q/\partial y - \partial q/\partial x\ \partial\psi/\partial y$ and

$$q = \nabla^2\psi - L_D^{-2}\psi \tag{4.17}$$

with $L_D^{-2} = f_0^2/c^2$, where $L_D$ is the deformation radius, also called the Rossby length or scale. Equation (4.14) is the evolution equation of the quasi-geostrophic potential vorticity $q$ in (4.15), alternatively given by (4.16) with (4.17). This evolution equation together with geostrophic balance relation (4.10) comprises the quasi-geostrophic model on an $f$-plane.

The quasi-geostrophic model illustrates the basic elements of any balanced model derived from the primitive equations. These elements are one evolution, or prognostic, equation and two balance, or diagnostic, relations. By comparison, the primitive equations have three evolution equations. Thus, in the case of both the primitive equations and any balanced model, the number of evolution equations is equal to the number of normal modes.

An alternative, shorter derivation of the quasi-geostrophic model, avoiding in particular the lengthy Fourier transformation from (4.13) to (4.14), is possible and especially beneficial for guiding the derivation of the equatorial balanced model in the next section. It is based on the fact that the general relation in terms of wavenumber space (4.12), and in the present case specific relation (4.13), is formally identical to its equivalent in physical space. This allows the derivation of the quasi-geostrophic model to be carried out entirely in physical space except for determining the eigenvalues.

To demonstrate this, we begin with determining the eigenvector of $\mathscr{L}$ in (3.5) that corresponds to the eigenvalue $\omega_R = 0$ in (4.4). It is easy to see that it is $\boldsymbol{y}_0^s$ as given by the second equation in (4.7). Eliminating $\psi(\boldsymbol{x}, t)$ leads to the geostrophic balance relation in (4.10). Guided by (4.13), we use the same $\boldsymbol{y}_0^s$, but as given by the first equation in (4.7), into the shallow water equations (3.3) and (3.4), apply the conjugate transpose of $\boldsymbol{e}_R(\boldsymbol{x})$ in (4.8) from the left, and thus obtain the quasi-geostrophic potential vorticity evolution equation in (4.14) with (4.15).

Salmon (1998, §2.10) shows that the derivation in wavenumber space presented in this section can be generalized to lead to the quasi-geostrophic model on a $\beta$-plane, i.e. $f = f_0 + \beta_y$, with a varying bottom. However, this is only possible by including the extra terms in the nonlinear term $\mathscr{N}$ in (3.5) despite the fact that the extra terms containing $\beta$ are linear. This illuminates the inconsistency that although $f$ is assumed to vary, the geostrophic balance relation of the quasi-geostrophic model on a $\beta$-plane is given in terms of the constant $f_0$.

## 5. Equatorial balanced model

The equatorial balanced model is derived on an equatorial $\beta$-plane in much the same way as the quasi-geostrophic model is derived on an $f$-plane in the previous section.

### 5.1. *Balance relations*

We first determine the eigenvalues and eigenvectors by solving (3.8) for $k = 0$ and (3.9) for $k \neq 0$, where in the present case we set $f = \beta y$. This creates the non-constant term $\omega(\beta y/c)^2$ in the bottom centre element of the matrix in (3.9). We therefore express $\boldsymbol{x}^s$ in (3.8) and (3.9) not in terms of its Fourier transform as in (4.1) but in terms of its Hermite transform, which takes the form

$$[\tilde{\boldsymbol{u}}(k, y, t), \tilde{\eta}(k, y, t)] = \sum_{m=0}^{\infty} [\hat{\boldsymbol{u}}_m(k, t), \hat{\eta}_m(k, t)]\, \phi_m(y'), \tag{5.1}$$

where $y' = \sqrt{\beta/c}\, y$ and $\phi_m(y')$ are the Hermite functions. They and their properties are described in appendix C. The resulting forms of (3.8) for $k=0$ and (3.9) for $k \neq 0$ are multiplied by $\phi_m(y')$ and integrated over all $y'$. Since $\phi_m(y')$ are orthonormal, as expressed in (C 3), we have for $k=0$,

$$\sum_{m=0}^{\infty} \begin{pmatrix} -\omega\delta_{n,m} & \mathrm{i}\beta b_{n,m} & 0 \\ -\mathrm{i}\beta b_{n,m} & -\omega\delta_{n,m} & -\mathrm{i}ca_{n,m} \\ 0 & -\mathrm{i}ca_{n,m} & -\omega\delta_{n,m} \end{pmatrix} \begin{pmatrix} \hat{u}_m(k,t) \\ \hat{v}_m(k,t) \\ \hat{\eta}_m(k,t) \end{pmatrix} = 0 \tag{5.2}$$

and for $k \neq 0$, using (C 9),

$$\sum_{m=0}^{\infty} \begin{pmatrix} \left[\left(\frac{\omega}{c}\right)^2 - k^2\right]\delta_{n,m} & \mathrm{i}ka_{n,m} - \mathrm{i}\frac{\beta}{c}\frac{\omega}{c}b_{n,m} & 0 \\ 0 & \mathrm{i}\frac{\omega}{c}a_{n,m} - \mathrm{i}\frac{\beta}{c}kb_{n,m} & \left[\left(\frac{\omega}{c}\right)^2 - k^2\right]\delta_{n,m} \\ 0 & \left[\left(\frac{\omega}{c}\right)^2 - k^2 - \frac{\beta k}{\omega} - (1+2n)\frac{\beta}{c}\right]\delta_{n,m} & 0 \end{pmatrix} \begin{pmatrix} \hat{u}_m(k,t) \\ \hat{v}_m(k,t) \\ \hat{\eta}_m(k,t) \end{pmatrix} = 0, \tag{5.3}$$

where

$$a_{n,m} = \int_{-\infty}^{\infty} \phi_n \frac{\partial \phi_m}{\partial y}\, \mathrm{d}y', \tag{5.4}$$

$$b_{n,m} = \int_{-\infty}^{\infty} \phi_n y \phi_m \, \mathrm{d}y' \tag{5.5}$$

and $\delta_{n,m}$ denotes the Kronecker delta.

The smallest eigenvalue of (5.2) and (5.3), respectively, is the frequency of the Rossby normal mode, denoted by $\omega_R$, which in the present case consists of the equatorial Rossby waves. The other two are the frequencies of the gravity normal modes, denoted by $\omega_{G\pm}$, consisting of equatorial gravity waves. For $n=0$, the equatorial Rossby and gravity waves are conventionally interpreted as mixed Rossby–gravity, or Yanai, wave and the westward-propagating Kelvin, or anti-Kelvin, wave. A fourth frequency is that of the Kelvin wave, given by $\omega_K = ck$ and depicted in figure 1. Because the Kelvin wave is characterized by $v=0$, its frequency cannot be obtained from (5.2) and (5.3) and thus must be derived separately (Gill 1982, § 11.5).

We are interested in the smallest eigenvalue $\omega_R$. For $k=0$, it is determined from (5.2), which gives $\omega_R = 0$. For $k<0$, it is one of the three solutions of the bottom centre matrix element in (5.3) set to zero, i.e. the dispersion relation, given by

$$\left(\frac{\omega}{c}\right)^2 - k^2 - \frac{\beta k}{\omega} - (1+2n)\frac{\beta}{c} = 0. \tag{5.6}$$

Solving for $k$, gives

$$k = -\frac{\beta}{2\omega} \pm \sqrt{\left(\frac{\omega}{c}\right)^2 + \frac{1}{4}\left(\frac{\beta}{\omega}\right)^2 - (1+2n)\frac{\beta}{c}}, \tag{5.7}$$

which allows the three solutions for the eigenvalue $\omega$ to be depicted as a function of $k$ and $n$ (Moore & Philander 1977). Figure 1 displays the smallest eigenvalue $\omega_R$ for $n=1,2,3$ as the solid curve labelled 1 and the two below it, respectively. Below them would be those for $n>3$. The other two solutions $\omega_{G\pm}$ for $n=1$ are displayed as one dashed-dotted curve, following the general convention of displaying negative $\omega$ for $k<0$ as positive $\omega$ for $k>0$. Above them would be those for $n>1$. A special case is $n=0$, whose three solutions are depicted by the two intersecting curves. The straight curve is the dispersion relation of the westward-propagating Kelvin wave

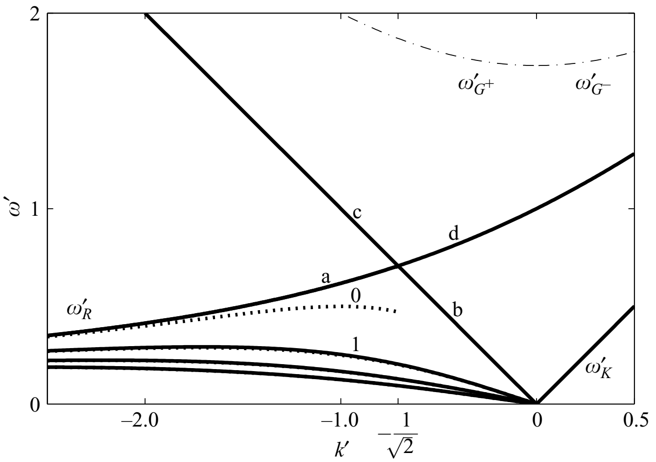


FIGURE 1. Dispersion relations. The axes show non-dimensionalized zonal wavenumber $k' = \sqrt{c/\beta}k$ and frequency $\omega' = \omega/\sqrt{\beta c}$. Equatorial Rossby waves for $n = 1, 2, 3$ correspond to the curves below the label 1, where the solid curves show the exact $\omega'_R$, given by (5.7) or iteration (5.8), and the dotted curves (hardly distinguishable from the solid curves) the approximate $\omega'_R$ in (5.13). The two intersecting curves represent the three solutions of (5.6) for $n = 0$. They define four parts, labelled a, b, c and d. Parts a and d correspond to the mixed Rossby–gravity, or Yanai, wave and parts c and b to the westward-propagating Kelvin, also called anti-Kelvin, wave. Alternatively, parts a and b correspond to the equatorial Rossby wave for $n = 0$ and parts c and d to the equatorial gravity wave for $n = 0$. Part a is approximated by the dotted curve labelled 0, which is given by the first iteration of (5.8) with $n = 0$. Equatorial gravity waves for $n = 1$ correspond to the dotted–dashed curve. The curve corresponding to the Kelvin wave is labelled by $\omega'_K$.

whose zonal velocity becomes unbounded for large $y$ and is therefore not physical (e.g. Pedlosky 1987, p. 678). The other curve is the dispersion relation of the mixed Rossby–gravity wave because it has the characteristics of an equatorial Rossby wave for $k \leqslant -\sqrt{\beta/c}/\sqrt{2}$ and that of a gravity wave for $k \geqslant -\sqrt{\beta/c}/\sqrt{2}$ (Matsuno 1966). These two intersecting curves offer an alternative interpretation suggested by Matsuno (1966), who points out that their intersection allows them to be split into four parts, labelled a, b, c and d in the figure. The curve made up of parts a and b has the shape of an equatorial Rossby wave dispersion relation and the curve made up of parts c and d has that of an equatorial gravity wave dispersion relation.

An explicit analytic expression for the smallest eigenvalue $\omega_R$ can be obtained by explicitly solving (5.6), which is a cubic equation in $\omega$ (e.g. Groove 2004, p. 278). The result, however, is too complicated to be used in the derivation of the equatorial balanced model. We therefore determine $\omega_R$ for all $n$, including the one for $n = 0$ depicted by the curve made up of parts a and b in figure 1, by re-writing (5.6) as

$$\omega^{[j+1]} = \frac{-\beta k}{k^2 + (1+2n)\beta/c - (\omega^{[j]}/c)^2}, \tag{5.8}$$

where $j$ is an index, setting $\omega^{[0]} = 0$, and iterating until $(\omega^{[j+1]} - \omega^{[j]}) \rightarrow 0$ (appendix D).

The eigenvector corresponding to the smallest eigenvalue $\omega_R$, and therefore spanning the Rossby manifold, is determined next. In (5.2) and (5.3), using (C 5) and (C 6), the coefficients $a_{n,m}$ and $b_{n,m}$ can be expressed as linear functions of $\delta_{n,m-1}$ and $\delta_{n,m+1}$ with constant coefficients, but not of $\delta_{n,m}$ only. This means that it is generally impossible to obtain a set of three linear equations for each value of $k$ and $n$ as it is possible for each value of $k$ and $l$ for the case of constant $f$ in the previous section. However, we can require that for each value of $n$, the eigenvector corresponding to the eigenvalue $\omega_R$ and given by (5.2) or (5.3) must have $\hat{\boldsymbol{u}}_m = \hat{\eta}_m = 0$ for all $m \neq n$. This allows (5.2) and (5.3) to be, respectively, expressed as a set of three equations, each of which has the form

$$\int_{-\infty}^{\infty} \phi_n \{\ldots\} \, \mathrm{d}y' = 0. \tag{5.9}$$

They are satisfied when the respective expressions in curly brackets are equal to zero. The resulting three equations for each value of $n$ determine the eigenvector and thus represent the balance relations.

For $k = 0$, the eigenvalue is $\omega_R = 0$ and the corresponding eigenvector satisfies (5.2), which, re-writing it in the form (5.9) and using (5.1), leads to

$$\bar{v}_R = 0, \tag{5.10}$$

$$\beta y \bar{u}_R = -c \frac{\partial \bar{\eta}_R}{\partial y}, \tag{5.11}$$

where $(\bar{\boldsymbol{u}}_R, \bar{\eta}_R) = [\tilde{\boldsymbol{u}}_R(0, y, t), \tilde{\eta}_R(0, y, t)]$. These equations are thus the balance relations defining the zonal average of the balanced flow to be a purely zonal flow that is in geostrophic balance.

For $k < 0$, the eigenvalue $\omega_R$ is one solution of (5.6), which can be shown to satisfy

$$\frac{(\omega_R/c)^2}{k^2} \leqslant \frac{1}{(1+2n)^2}. \tag{5.12}$$

For $n \geqslant 1$, the ratio on the left-hand side is smaller than 1/9 and therefore we can neglect $(\omega_R/c)^2$ in the top left and centre right matrix elements in (5.3). Furthermore, in the top and centre elements of the centre column, we do not insert the exact eigenvalue $\omega_R$ but an approximation to it, given by the first step of the iteration in (5.8), i.e.

$$\omega_R = \frac{-\beta k}{k^2 + (1+2n)\,\beta/c}. \tag{5.13}$$

This approximate $\omega_R$ for $n = 1, 2, 3$ is depicted by the dotted curves in figure 1, which can hardly be distinguished from the solid curve labelled 1 and the two below it, depicting the corresponding exact $\omega_R$. The upper bound of the error, defined by $\epsilon = (\omega_R^e - \omega_R)/\omega_R^e$, where '$e$' is used to denote the exact $\omega_R$, is only $\epsilon = 0.02$, therefore justifying the approximation in (5.13). For $n = 0$, we partition negative $k$ into two intervals. For $k \leqslant -\sqrt{\beta/c}/\sqrt{2}$, figure 1 shows that as $k$ increases towards $-\sqrt{\beta/c}/\sqrt{2}$, the dispersion relation changes from one of the equatorial Rossby waves into one of the equatorial gravity waves and the ratio on the left-hand side of (5.12) monotonically increases towards 1. This motivates to replace the exact $\omega_R$, as for $n \geqslant 1$ above, by the approximate $\omega_R$ in (5.13), shown by the dotted curve labelled 0 in figure 1. Thus, the dispersion relation has the shape of one of the equatorial Rossby waves and the ratio on the left-hand side of (5.12) only increases towards 4/9. The upper bound of the error in the $n = 0$ case is $\epsilon = 0.33$, indicating that the approximation is not as good as that for $n \geqslant 1$. The effects of this approximation are discussed in § 5.3. For $-\sqrt{\beta/c}/\sqrt{2} \leqslant k < 0$, the exact eigenvalue is $\omega_R = -ck$.

Implementing all of the above, we rewrite (5.3) in form (5.9), set the expression in the curly brackets to zero, replace $m$ with $n$ and multiply the resulting equations by $-\mathrm{i}\beta$ and divide them by $\omega_R$ in (5.13). For $k < 0$ and all $n$, except for $-\sqrt{\beta/c}/\sqrt{2} \leqslant k < 0$

and $n=0$, the eigenvector corresponding to the eigenvalue $\omega_R$ in (5.13) thus satisfies

$$\sum_{n=0}^{\infty}\left[\mathrm{i}k\hat{D}\left(\hat{u}_n\phi_n\right)+\left(\hat{D}\frac{\partial}{\partial y}-\frac{\beta^2}{c^2}y\right)\left(\hat{v}_n\phi_n\right)\right]=0, \tag{5.14}$$

$$\sum_{n=0}^{\infty}\left[\frac{\beta}{c}\left(\frac{\partial}{\partial y}-\hat{D}y\right)\left(\hat{v}_n\phi_n\right)+\mathrm{i}k\hat{D}\left(\hat{\eta}_n\phi_n\right)\right]=0, \tag{5.15}$$

where

$$\hat{D}=-k^2-(1+2n)\frac{\beta}{c}. \tag{5.16}$$

For the interval $-\sqrt{\beta/c}/\sqrt{2}\leqslant k<0$ for $n=0$, the above leads to $\hat{v}_n=0$ and arbitrary values for $\hat{u}_n$ and $\hat{\eta}_n$, which we set to zero.

Hermite- and Fourier transforming (5.14) and (5.15) with (5.16), as specified by (5.1) and (3.7), respectively, and using (C 9), leads to

$$\frac{\partial}{\partial x}Du'_R+\frac{\partial}{\partial y}Dv'_R-\frac{\beta^2}{c^2}yv'_R=0, \tag{5.17}$$

$$\frac{\beta}{c}\frac{\partial}{\partial y}v'_R-\frac{\beta}{c}yDv'_R+\frac{\partial}{\partial x}D\eta'_R=0, \tag{5.18}$$

where

$$D=\left(\frac{\partial^2}{\partial x^2}+\frac{\partial^2}{\partial y^2}-\frac{\beta^2}{c^2}y^2\right) \tag{5.19}$$

is the modified Helmholtz operator and the primes denote perturbations from the zonal mean. These equations are thus the balance relations defining the perturbation from the zonal mean flow of the balanced flow. An immediate implication is that they do not permit a Kelvin wave. This is because a Kelvin wave is characterized by $v'_R=0$, for which (5.17) and (5.18) give $u'_R=\eta'_R=0$.

In the context of the geometric framework described in § 2, a vector on the Rossby manifold is in the present case given by

$$\boldsymbol{y}_0^s=(\boldsymbol{u}_R,\eta_R)=\bar{\boldsymbol{y}}_0^s+\boldsymbol{y}'^s_0, \tag{5.20}$$

which can be expressed equivalently to (4.7) in terms of a function, whose zonal mean and perturbation are, respectively, denoted by $\bar{\Psi}$ and $\Psi'$, as

$$\bar{\boldsymbol{y}}_0^s=(\bar{\boldsymbol{u}}_R,\bar{\eta}_R)=\bar{\boldsymbol{e}}_R(\boldsymbol{x})\bar{\Psi}(\boldsymbol{x},t), \tag{5.21}$$

$$\boldsymbol{y}'^s_0=(\boldsymbol{u}'_R,\eta'_R)=\boldsymbol{e}'_R(\boldsymbol{x})\Psi'(\boldsymbol{x},t). \tag{5.22}$$

To determine $\bar{\boldsymbol{e}}_R$, we write (5.10) and (5.11) in the form

$$\bar{\boldsymbol{e}}^{\dagger}_{G^1}\cdot\bar{\boldsymbol{y}}_0^s=0, \tag{5.23}$$

$$\bar{\boldsymbol{e}}^{\dagger}_{G^2}\cdot\bar{\boldsymbol{y}}_0^s=0, \tag{5.24}$$

which implies because of (5.21) that we must have

$$\bar{\boldsymbol{e}}^{\dagger}_{G^1}\cdot\bar{\boldsymbol{e}}_R=\bar{\boldsymbol{e}}^{\dagger}_{G^2}\cdot\bar{\boldsymbol{e}}_R=0. \tag{5.25}$$

We therefore obtain

$$\bar{\boldsymbol{e}}_R = \begin{pmatrix} -\frac{\partial}{\partial y} \\ 0 \\ \frac{\beta}{c}y - \frac{\beta}{c}\left(\frac{\partial}{\partial y}\right)^{-1} \end{pmatrix}; \quad \bar{\boldsymbol{e}}_{G^1} = \begin{pmatrix} 0 \\ -\frac{\partial}{\partial y} \\ 0 \end{pmatrix}; \quad \bar{\boldsymbol{e}}_{G^2} = \begin{pmatrix} 0 \\ -\frac{\beta}{c}y - \frac{\beta}{c}\left(\frac{\partial}{\partial y}\right)^{-1} \\ 0 \end{pmatrix}. \tag{5.26}$$

To determine $\boldsymbol{e}'_R$, we multiply (5.17) and (5.18) on the left by $D^{-1}$. The result is then rewritten as (5.10) and (5.11), leading to

$$\boldsymbol{e}'_R = \begin{pmatrix} -\frac{\partial}{\partial y} + 3\frac{\beta^2}{c^2}D^{-1}y \\ \frac{\partial}{\partial x} \\ \frac{\beta}{c}y - 3\frac{\beta}{c}D^{-1}\frac{\partial}{\partial y} \end{pmatrix}; \quad \boldsymbol{e}'_{G^1} = \begin{pmatrix} -\frac{\partial}{\partial x} \\ -\frac{\partial}{\partial y} - 3\frac{\beta^2}{c^2}D^{-1}y \\ 0 \end{pmatrix}; \quad \boldsymbol{e}'_{G^2} = \begin{pmatrix} 0 \\ -\frac{\beta}{c}y - 3\frac{\beta}{c}D^{-1}\frac{\partial}{\partial y} \\ -\frac{\partial}{\partial x} \end{pmatrix}. \tag{5.27}$$

These vectors are analogous to those in (4.5) and in particular $\bar{\boldsymbol{e}}_R$ and $\boldsymbol{e}'_R$ are also analogous to $\boldsymbol{e}_R$ in (4.8). In this case, however, they cannot be normalized and are therefore not marked by a hat. As expressed by (5.25), which is also the case for the primed vectors, the vectors with subscripts $G^1$ and $G^2$ are orthogonal to that with subscript $R$ in both cases. However, they are not mutually orthogonal. For this reason, we have used $G^1$ and $G^2$ to distinguish them from the mutually orthogonal ones with subscripts $G^{\pm}$ in (4.5).

### 5.2. *Evolution equation*

The equatorial balanced model, as any other balanced model, has two components: the balance relations derived in the previous section and an evolution equation derived in this section. In the geometric framework described in § 2, the evolution equation is given by (2.4). We use (2.4) in its rewritten, more practical form (4.12) in which $\boldsymbol{e}_R$ represents both $\bar{\boldsymbol{e}}_R$ in (5.26) and $\boldsymbol{e}'_R$ in (5.27). For the equatorial balanced model, (4.12) takes a complicated form. It can, however, be substantially simplified by making two approximations that are justified *a posteriori*.

The first approximation is to replace $\boldsymbol{e}_R^{\dagger}$ by

$$\boldsymbol{e}_{Ra}^{\dagger} = \left(\frac{\partial}{\partial y}, -\frac{\partial}{\partial x}, \frac{\zeta_R + \beta y}{c + \eta_R}\right), \tag{5.28}$$

where $\zeta_R = \nabla \times \boldsymbol{u}_R$. While $\boldsymbol{e}_R$ spans the Rossby manifold, $\boldsymbol{e}_{Ra}$ can be thought of spanning an approximate Rossby manifold. The close relation between $\boldsymbol{e}_R$ and $\boldsymbol{e}_{Ra}$ is apparent, especially by noting that the linear form of the third element of $\boldsymbol{e}_{Ra}$ is $(\beta/c)y$. This first approximation means that the evolution of a single point on the approximate slow manifold described by (2.3) is not projected onto the Rossby manifold leading to (4.12), but onto the approximate Rossby manifold leading to (4.12) with $\boldsymbol{e}_R^{\dagger}$ replaced by $\boldsymbol{e}_{Ra}^{\dagger}$. Its linear terms thus take the form

$$\boldsymbol{e}_{Ra}^{\dagger} \cdot \dot{\boldsymbol{x}}^s = \boldsymbol{e}_{Ra}^{\dagger} \cdot (\dot{\boldsymbol{y}}_0 + \dot{z}_1), \tag{5.29}$$

$$-\mathrm{i}\boldsymbol{e}_{Ra}^{\dagger} \cdot \mathscr{L}\boldsymbol{x}^s = -\mathrm{i}\boldsymbol{e}_{Ra}^{\dagger} \cdot \mathscr{L}(\boldsymbol{y}_0 + z_1), \tag{5.30}$$

where $\boldsymbol{x}^s = \boldsymbol{y}_0 + z_1$ is a vector in the approximate slow manifold, as derived in § 2. The second approximation is to neglect the terms depending on $z_1$ in (5.29) and (5.30). The result of both approximations thus is that (4.12) simplifies to

$$\boldsymbol{e}_{Ra}^{\dagger} \cdot \dot{\boldsymbol{y}}_0^s = -\mathrm{i}\boldsymbol{e}_{Ra}^{\dagger} \cdot \mathscr{L}\boldsymbol{y}_0^s + \boldsymbol{e}_{Ra}^{\dagger} \cdot \mathscr{N}(\boldsymbol{y}_0^s). \tag{5.31}$$

To assess the degree of accuracy of these two approximations, we compare the linear forms of (5.31) and (4.12). The linear form of the latter is identical to the linear form of the shallow water equations (2.1) multiplied from the left by $\boldsymbol{e}_R^\dagger$. Thus, the comparison is between the linear dynamics described by the equatorial balanced model and the low-frequency component of the linear dynamics described by the shallow water equations. Their respective dispersion relations are compared below, which shows that the dispersion relation of the equatorial balanced model approximates that of the shallow water equations strikingly well. This implies that the above two approximations minimally change the linear dynamics and in particular that $\boldsymbol{e}_{Ra}$ is a good approximation of $\boldsymbol{e}_R$, which in turn implies that the nonlinear terms are also approximated well.

The form of (5.31) is equivalent to that of (4.13). As pointed out in the second paragraph below (4.17), (4.13) is independent of a particular space and the simplest path from (4.13) to (4.14) with (4.15) turns out to be that taken entirely in physical space. The same applies to (5.31) and therefore we take the equivalent path in physical space. This means we note that $\boldsymbol{y}_0^s$ is given by the first equation in (5.20) and substitute it for $(\boldsymbol{u}, \eta)$ in (3.3) and (3.4) with $f = \beta y$ and multiply the result from the left by $\boldsymbol{e}_{Ra}^\dagger$ in (5.28). In this way, we determine the individual terms separately, which become

$$\boldsymbol{e}_{Ra}^\dagger \cdot \dot{\boldsymbol{y}}_0^s = -(c+\eta_R)\frac{\partial}{\partial t}\left(\frac{\zeta_R + \beta y}{c+\eta_R}\right) \tag{5.32}$$

$$\boldsymbol{e}_{Ra}^\dagger \cdot \mathscr{L}\boldsymbol{y}_0^s = \boldsymbol{u}_R \cdot \nabla(\beta y) + \beta y \nabla \cdot \boldsymbol{u}_R - \frac{\zeta_R + \beta y}{c+\eta_R} c \nabla \cdot \boldsymbol{u}_R \tag{5.33}$$

$$\boldsymbol{e}_{Ra}^\dagger \cdot \mathscr{N}\left(\boldsymbol{y}_0^s\right) = \boldsymbol{u}_R \cdot \nabla \zeta_R + \zeta_R \nabla \cdot \boldsymbol{u}_R + \frac{\zeta_R + \beta y}{c+\eta_R}\left[-\boldsymbol{u}_R \cdot \nabla(c+\eta_R) - \eta_R \nabla \cdot \boldsymbol{u}_R\right]. \tag{5.34}$$

Thus, (5.31) becomes

$$\frac{\partial q}{\partial t} + \boldsymbol{u}_R \cdot \nabla q = 0, \tag{5.35}$$

where $q$ is the potential vorticity, given by

$$q = \frac{\zeta_R + \beta y}{c + \eta_R}. \tag{5.36}$$

The evolution equation of the equatorial balanced model is therefore the material conservation of potential vorticity.

### 5.3. *Dispersion relation*

We derive the dispersion relation of the equatorial balanced model in particular to understand and justify some of the approximations made in its derivation. Linearizing (5.35) gives

$$\frac{\partial}{\partial t}\left(\zeta_R - \frac{\beta y}{c}\eta_R\right) = -v_R \beta. \tag{5.37}$$

The zonal average of the left-hand side of (5.37) vanishes because of (5.10). Using this after substituting the second equation in (5.20) with (5.21) and (5.22), where $\bar{\boldsymbol{e}}_R$ and $\boldsymbol{e}_R'$ are given by (5.26) and (5.27), into (5.37), gives

$$\frac{\partial}{\partial t}\left[D + 3\frac{\beta^2}{c^2}\left(y D^{-1}\frac{\partial}{\partial y} - \frac{\partial}{\partial y}D^{-1}y\right)\right]\Psi' = -\beta\frac{\partial \Psi'}{\partial x}. \tag{5.38}$$

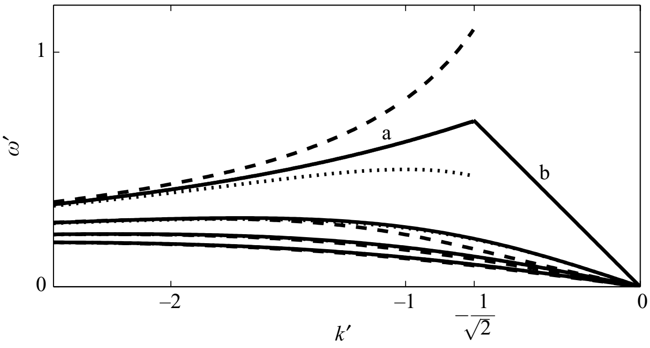


FIGURE 2. Dispersion relations of the equatorial balanced model with $\alpha = 0$ (dashed curves). The other curves (solid and dotted) are identical to those in figure 1 and are displayed for comparison.

We take $\Psi'$ to have the form of a harmonic wave in the $x$-direction, given by

$$\Psi' \propto \phi_n(y')\mathrm{e}^{\mathrm{i}kx-\mathrm{i}\omega t}, \tag{5.39}$$

where $k<0$ and $y' = \sqrt{\beta/c}\,y$ as before. Using (C 5), (C 6) and (C 10), allows to show that

$$\left(yD^{-1}\frac{\partial}{\partial y} - \frac{\partial}{\partial y}D^{-1}y\right)\phi_n(y')\mathrm{e}^{\mathrm{i}kx} = \left\{\frac{n+1}{k^2+[1+2(n+1)]\,\beta/c} - \frac{n}{k^2+[1+2(n-1)]\,\beta/c}\right\}\phi_n(y')\mathrm{e}^{\mathrm{i}kx}. \tag{5.40}$$

Substituting (5.39) and (5.40) into (5.38), leads to the dispersion relation of the equatorial balanced model,

$$\omega = \frac{-\beta k}{k^2+(1+2n)\beta/c - 3\beta^2/c^2\left[\dfrac{n+1}{k^2+(2n+3)\,\beta/c} - \dfrac{n}{k^2+(2n-1)\,\beta/c}\right]}. \tag{5.41}$$

Figure 2 depicts (5.41) as dashed curves. The solid and dotted curves are identical to those in figure 1 and included for comparison. For $n=2$, 3, dispersion relation (5.41) (bottom two dashed curves) approximates well that of the shallow water equations (bottom two solid curves). The approximation is even better for $n \geqslant 4$ (not shown). This justifies for $n \geqslant 2$ the approximation made in the derivation of the equatorial balanced model. However, the top two dashed curves indicate that the equatorial balanced model fails to approximate well the dispersion relation of the Rossby-wave part of the Rossby–gravity wave and the equatorial Rossby wave for $n=1$ of the shallow water equations (top solid curve labelled a and the solid curve below it, respectively). This shortcoming is resolved by a generalization of the equatorial balanced model, which is presented in the next section.

### 5.4. *Generalization*

To obtain an equatorial balanced model that better approximates the Rossby-wave part of the mixed Rossby–gravity wave corresponding to the solid curve labelled a in figure 2 than that corresponding to the top dashed curve, we generalize its derivation. This is achieved by generalizing the approximation to the smallest eigenvalue $\omega_R$ in (5.13) by replacing $2n$ by $2n+\alpha$, where $\alpha$ is a free parameter. This amounts to a change in the first guess used in the iterative solution (5.8). The only constraint on $\alpha$

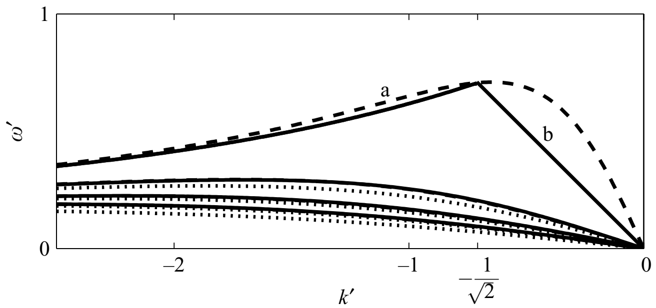


FIGURE 3. Dispersion relations of the equatorial balanced model with $\alpha = 2.5$ (top dashed curve and the three dashed curves below it, which are overlaid by the bottom three solid curves). The dotted curves are the approximations of $\omega_R$ as given by (5.13) for $n = 0, 1, 2, 3$, respectively, from top to bottom with $2n$ replaced by $2n + \alpha$, where $\alpha = 2.5$. The solid curves are identical to those in figure 1 and displayed for comparison.

is that the first guess $\omega_R$ resulting from the replacement of $2n$ by $2n + \alpha$ should allow the iteration to converge to the exact $\omega_R$ given by (5.6). The introduction of $\alpha$ only affects $\hat{D}$ in (5.16), which generalizes to

$$\hat{D}_\alpha = -k^2 - (1 + 2n + \alpha)\frac{\beta}{c}, \tag{5.42}$$

and consequently its form in physical space, given for $\alpha = 0$ by $D$ in (5.19), becomes the redefined modified Helmholtz operator

$$D_\alpha = \left(\frac{\partial^2}{\partial x^2} + \frac{\partial^2}{\partial y^2} - \frac{\beta^2}{c^2}y^2 - \frac{\beta}{c}\alpha\right). \tag{5.43}$$

With this change, dispersion relation (5.41) of the equatorial balanced model generalizes to

$$\omega = \frac{-\beta k}{k^2 + (1 + 2n)\beta/c - 3\beta^2/c^2\left[\dfrac{n+1}{k^2 + (2n + 3 + \alpha)\beta/c} - \dfrac{n}{k^2 + (2n - 1 + \alpha)\beta/c}\right]}. \tag{5.44}$$

The parameter $\alpha$ allows us to adjust the dispersion relation of the equatorial balanced model to better fit that of the shallow water equations, in particular regarding that of the Rossby-wave part of the mixed Rossby–gravity wave. A good adjustment is achieved by simply requiring $\omega$ in (5.44) with $n = 0$ to have the same value as $\omega$ of the mixed Rossby–gravity wave of the shallow water equations at $k = -\sqrt{\beta/c}/\sqrt{2}$, which is given by $\omega = \sqrt{\beta c}/\sqrt{2}$. We thus obtain $\alpha = 2.5$. We have, however, the freedom to set $\alpha$ to a different value in order to approximate better other desirable properties of the shallow water equations.

Figure 3 depicts the same dispersion relations as figure 2 but for $\alpha = 2.5$ instead of $\alpha = 0$. The dispersion relation of the Rossby-wave part of the mixed Rossby–gravity wave of the equatorial balanced model (top dashed curve) approximates well that of the shallow water equations (solid curve labelled a). A strikingly accurate approximation is achieved by (5.44) for the dispersion relation of the equatorial Rossby waves, indistinguishable from that of the shallow water equations (the three bottom dashed curves are overlaid with the three bottom solid curves). This result justifies the cruder approximation compared to that for $\alpha = 0$ as manifested by the differences between the respective dotted and solid curves in figures 2 and 3.

When compared with figure 2, the top dotted and dashed curves for $n=0$ in figure 3 extend to $k=0$. This represents an alternative to the part of the derivation concerning the interval $-\sqrt{\beta/c}/\sqrt{2}\leqslant k<0$ for the case $n=0$. This part of the derivation, described below (5.13), uses the exact solution $\omega_R=-ck$, labelled as b, for the smallest eigenvalue, which implies that $\hat{v}_0=0$ and $\hat{u}_0$ and $\hat{\eta}_0$ are arbitrary and therefore we set them to zero as a convention. The alternative is to approximate the exact solution. This is possible because of the introduction of the parameter $\alpha$. The approximation is given by (5.13) in its generalized form, where $2n$ is replaced by $2n+\alpha$. Relation (5.12) would then for the particular case of $n=0$ becomes $(\omega_R/c)^2/k^2\leqslant 1/(1+\alpha)^2$, justifying that $(\omega_R/c)^2$ can be neglected compared with $k^2$ in the present case of $\alpha=2.5$. As a result, we obtain the extension of the top dashed curve from $k=-\sqrt{\beta/c}/\sqrt{2}$ to $k=0$, $\hat{v}_0$ is generally non-zero, and $\hat{u}_0$ and $\hat{\eta}_0$ are not arbitrary. This extension of the curve can be considered to be an approximation to the dispersion relation of the westward-propagating Kelvin wave, given by the solid curve labelled b, or, because of its characteristics, the dispersion relation of an additional equatorial Rossby wave not described by the shallow water equations.

### 5.5. *Summary of the equatorial balanced model*

The equatorial balanced model consists of the evolution equation of potential vorticity (5.35) with (5.36) and two balance relations, respectively, for the zonal mean flow, given by (5.10) and (5.11), and the perturbation from the zonal mean flow, given by (5.17) and (5.18), where $D$ is replaced by the more general term $D_\alpha$ in (5.43) with $\alpha$ being a free parameter. In order to obtain an accurate dispersion relation we suggest $\alpha=2.5$. The dispersion relation is given by (5.44). It is depicted in figure 3 (dashed curves) and approximates the corresponding parts of that of the shallow water equations (solid curves) strikingly well.

## 6. Limits

In certain limits the equatorial balanced model takes simpler forms. To this end, we non-dimensionalize the balance relations in the form of (5.14) and (5.15) with $\hat{D}$ generalized to $\hat{D}_\alpha$ in (5.42) using the scaling

$$k=\sqrt{\frac{\beta}{c}}k';\quad y=\sqrt{\frac{c}{\beta}}y';\quad \omega_R=\sqrt{\beta c}\,\omega_R', \tag{6.1}$$

where $\sqrt{c/\beta}$ defines the size of the equatorial deformation radius, also called the equatorial Rossby length or scale,

$$\omega_R'=\frac{-k'}{k'^2+1+2n+\alpha}, \tag{6.2}$$

and the primes denote non-dimensional variables. Furthermore, we assume an identical scaling for $\hat{u}_n\phi_n$, $\hat{v}_n\phi_n$ and $\hat{\eta}_n\phi_n$, which is possible because $\eta$ has the dimension of velocity as pointed out above (3.3). The balance relations thus take the form

$$\sum_{n=0}^{\infty}\left[(\hat{u}_n'\phi_n')+\left(-\mathrm{i}\frac{1}{k'}\frac{\partial}{\partial y'}+\mathrm{i}\frac{\omega_R'y'}{k'^2}\right)(\hat{v}_n'\phi_n')\right]=0, \tag{6.3}$$

$$\sum_{n=0}^{\infty}\left[\mathrm{i}\left(\frac{\omega_R'}{k'^2}\frac{\partial}{\partial y'}-\frac{y'}{k'}\right)(\hat{v}_n'\phi_n')-(\hat{\eta}_n'\phi_n')\right]=0. \tag{6.4}$$

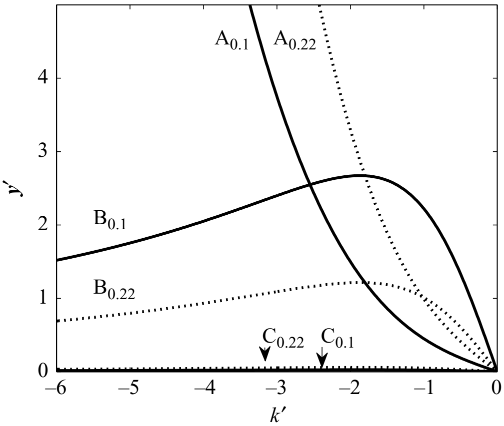


FIGURE 4. Limits: the curves labelled A, B and C are the right-hand sides of (6.5), (6.8) and (6.10), respectively, where the subscripts indicate the values of $\epsilon$.

### 6.1. *Scale analysis*

We assume isotropy and thus we can apply $\partial/\partial y' \approx k'$. We first consider balance relation (6.3). Its third term can be neglected if the condition,

$$y' < \epsilon[-k'(k'^2 + 1 + \alpha)] \tag{6.5}$$

is satisfied, where $\epsilon$ is a parameter chosen to be sufficiently smaller than 1. If this is the case the balance relation does not become (5.17), but instead

$$\nabla \cdot \boldsymbol{u}'_R = 0, \tag{6.6}$$

where, as in (5.17), the variables are dimensional and the primes indicate a perturbation from the zonal mean flow. This implies that (5.22) is given in terms of $\boldsymbol{e}'_R$ in (5.27) with the second term in the top element neglected. By substituting (5.22) in this particular form into the other balance relation (5.18) with $D$ replaced by the more general term $D_\alpha$ in (5.43), it simplifies to

$$\beta y D_\alpha \psi - \beta \frac{\partial \psi}{\partial y} - c D_\alpha \eta'_R = 0. \tag{6.7}$$

For all negative $k'$, the range of $y'$ satisfying condition (6.5) covers the area between the curves labelled A and the negative $k'$ axis in figure 4, where the subscripts of A denote the values of $\epsilon$. It shows that (6.6) is valid in the equatorial region and beyond it, except for small negative $k'$ for which it only remains valid within a latitudinal band around the equator whose width decreases with decreasing $|k'|$.

Using the simple balance relation (6.6) in place of (5.17) is expected to alter the dispersion relation of the equatorial balanced model. To determine its altered form, we substitute (5.22) in the above particular form into (5.37). This leads to (5.38) without the third term on its left-hand side. In the generalized case, the $D^{-1}$ operator in the second term on the left-hand side becomes $D_\alpha^{-1}$, but the operator $D$ remains unchanged. We then insert $\psi'(\boldsymbol{x}, t) = \hat{\psi}'(y)\exp(\mathrm{i}kx - \mathrm{i}\omega t)$, use (6.1), expand $\hat{\psi}'$ in terms of Hermite functions similarly to (5.1), use (C 5), (C 6) and (C 8), multiply by $\phi_m$, use (C 3), and truncate the series. This procedure leads to an eigenvalue problem with the eigenvalues of the form $k'/\omega'_R$, which can be solved numerically. The dispersion relation thus obtained is shown by the dashed curves in figure 5. They should be compared with the dashed curves in figure 3, showing the dispersion

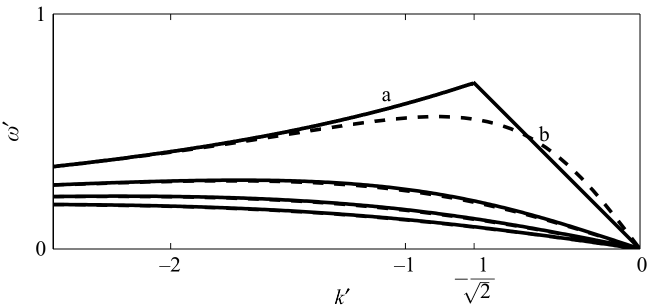


FIGURE 5. Dispersion relation of the equatorial balanced model with $\alpha = 2.5$ and approximation (6.6) (dashed curves of which the bottom three are overlaid with the bottom three solid curves). The solid curves are identical to those in figure 1 and are displayed for comparison.

relation without the above simplification. The dispersion relation is altered minimally by the simplification, except in the case of the Rossby-wave part of the mixed Rossby–gravity wave for about $-1.5 < k' \leqslant 0$. This is, however, consistent with the condition that the simple balance relation (6.6) is valid only within a latitudinal band around the equator whose width decreases with decreasing $|k'|$.

The other balance relation (6.4) can be considered similarly. Its first term can be neglected if the condition,

$$y' > \frac{1}{\epsilon} \frac{-k'}{k'^2 + 1 + \alpha}, \tag{6.8}$$

is satisfied and in this particular case the scale for the meridional velocity $\hat{v}_n$ is set to be of order $\epsilon \hat{\eta}_n$. If this is the case, the balance relation does not become (5.18), but instead

$$\beta y v'_R = c \frac{\partial \eta'_R}{\partial x}, \tag{6.9}$$

which is the expression of geostrophic balance in the zonal direction. This implies that (5.22) is given in terms of $\boldsymbol{e}'_R$ in (5.27) with the second term in the bottom element neglected. For all negative $k'$, the range of $y'$ satisfying (6.8) covers the area above the curves labelled B in figure 4, where the subscripts of B denote the values of $\epsilon$.

Figure 4 indicates that both (6.6) and (6.9) are valid sufficiently far away from the equator if $|k'|$ is sufficiently large, i.e. above a curve labelled B and below a curve labelled A. If they are both valid, (5.22) is given in terms of $\boldsymbol{e}'_R$ in (5.27) with both second terms in the top and bottom elements neglected. Substituting (5.20) with this particular form of (5.22) into (5.35) and assuming a case of no zonal mean flow and that $q$ can be linearized, we obtain (4.16) with $q = \nabla^2\psi - L_D^{-2}\psi + \beta y$, where $L_D^{-2} = (\beta y)^2/c^2$. This is exactly the modified form of the quasi-geostrophic model on a $\beta$-plane introduced by Salmon (1982, 1998, p. 284) and further studied by Theiss (2004, equation (1)). It is considered modified because $L_D$ is $y$-dependent instead of constant. A $y$-dependent $L_D$, however, is more natural for a $\beta$-plane and generally more realistic.

Instead of neglecting the first term in the other balance relation (6.4) as above, the second term can be neglected if instead of (6.8) the condition

$$y' < \epsilon \frac{-k'}{k'^2 + 1 + 2n + \alpha} \tag{6.10}$$

is satisfied. If this is the case, condition (6.5) is also satisfied and thus, using (6.6), the balance relation (6.4) becomes,

$$\beta u'_R = cD_\alpha \eta'_R \tag{6.11}$$

instead of (5.18). For all negative $k'$, the range of $y'$ satisfying (6.10) with $n=0$ covers the area below the curves labelled C and the negative $k'$-axis, where the subscripts of C denote the values of $\epsilon$. For all negative $k'$, the range of $y'$ decreases with increasing $n$. It is, however, possible to increase the range of $y'$ and thus the range of validity of (6.11) if we assume anisotropy with lengths scales being larger in the zonal than the meridional direction, i.e. we can assume $\partial/\partial y \approx rk$ with $r > 1$. Consequently, in (6.5) and (6.10) $\epsilon$ is multiplied by $r$, thereby increasing the range of $y'$.

### 6.2. *Asymptotic analysis*

The same limits as given above can be obtained from an asymptotic analysis, which provides further insight. From (5.6) we determine the frequency of the gravity normal modes at $k=0$ and $n=0$ to be $\omega_{G\pm} = \sqrt{\beta c}$. This permits us to express $\omega_R$ in (6.1) as $\omega_R = \epsilon\sqrt{\beta c}\,\omega''_R$, where

$$\epsilon = \frac{\omega_R}{\omega_{G\pm}}. \tag{6.12}$$

The maximum of $\omega_R$ in (5.13) is at $k = -\sqrt{(1+\alpha)\beta/c}$ and $n=0$, which gives us an upper bound of $\epsilon = 0.27$ for $\alpha = 2.5$. Assuming that $k'$, $y'$ and $\omega''_R$ are of order unity and substituting the expansion in powers of $\epsilon$ given by

$$\left[(\hat{u}'_n\phi'_n), (\hat{v}'_n\phi'_n), (\hat{\eta}'_n\phi'_n)\right] = \sum_{p=0}^{\infty} \left[(\hat{u}'_n\phi'_n)_p, (\hat{v}'_n\phi'_n)_p, (\hat{\eta}'_n\phi'_n)_p\right] \epsilon^p, \tag{6.13}$$

into (6.3) and (6.4), shows that the first and second terms in (6.3) and the second and third terms in (6.4) are of leading order. The leading-order solution is thus, rewritten as above, given by (6.6) and (6.9). This is consistent with the above scale analysis because $\epsilon = 0.27 > 0.22$, where 0.22 is the smallest value of $\epsilon$ necessary for the case considered here, i.e. $(k', y') = (-1, 1)$, to lie below a curve $A_\epsilon$ and above a curve $B_\epsilon$ in figure 4.

To carry out the asymptotic analysis in the vicinity of the equator, we assume $y' = \epsilon y''$ with $y''$ being of order unity. Repeating the same procedure, the leading-order solution becomes (6.6) and (6.11). The different scaling of $y$ implies that we are assuming the length scale in the $y$-direction to be of order $\epsilon$. In this respect as well, there is consistency between the asymptotic and the scale analyses. Because of the different scaling $r = 1/\epsilon$, which has the effect that $\epsilon$ in (6.5) and (6.10) is replaced by 1, and therefore $(k', y') = (-1, \epsilon)$ satisfies (6.5) and (6.10) (not shown in figure 4).

We refer to (6.9) and (6.11) as the outer and inner solutions, respectively. To determine the inner limit of the outer solution, we consider the leading-order terms in (6.4) with (6.13), which is equivalent to (6.9), then substitute $y' = \epsilon y''$, and take the limit $\epsilon \to 0$ while keeping $y''$ fixed. Similarly, to determine the outer limit of the inner solution, we consider the leading-order terms in (6.4) with (6.13) and $y' = \epsilon y''$, which is equivalent to (6.11), then substitute $y'' = y'/\epsilon$, and take the limit $\epsilon \to 0$ while keeping $y'$ fixed. Both limits are zero. Thus, $\eta'_R$ is given in terms of $v'_R$ in (5.18) and can be considered as a composite leading-order solution combining (6.9) and (6.11).

## 7. Extensions

The equatorial balanced model, as summarized in § 5.5, describes the balanced dynamics of an unforced shallow layer of fluid with constant density on an infinite equatorial $\beta$-plane. Extending it so that it can also describe the balanced dynamics of bounded, forced and stratified fluids requires only minor changes to its derivation.

### 7.1. *Boundaries*

A widely used configuration is a channel that is periodic in the zonal direction and bounded by solid zonal boundaries in the meridional direction. This implies $v = 0$ at these boundaries. In the derivation of the equatorial balanced model for the meridionally unbounded case in this paper, $v$ as well as $u$ and $\eta$ are expressed in (3.7) with (5.1) in terms of Hermite functions $\phi_n$. This enables the use of relation (C 8), which can be considered an eigenvalue problem with the eigenvalues $2n+1$ and the eigenfunctions being the Hermite functions. For the meridionally bounded case with the boundary condition $v = 0$, the eigenvalue problem (C 8) remains the same, except that in place of the integer $n$, a real number $\mu_n$ must be assumed. This eigenvalue problem is solved analytically by Cane & Sarachik (1979). They show that the eigenvalues $\mu_n$ do not differ much from $n$, as also noted by Gent & McWilliams (1983), and that the eigenfunctions are not the Hermite functions, but similar and also a complete orthonormal set. The equatorial balanced model for the meridionally bounded case can therefore be derived by complete analogy to the meridionally unbounded case. Between the two cases, only the eigenvalues and eigenfunctions differ and thus only the transformations of form (5.1) differ. This implies that in physical space the respective derivations and the resulting equatorial balanced models for both cases are formally identical.

Their respective dispersion relations, however, differ because of the differing eigenvalues of $n$ and $\mu_n$. Furthermore, an analytical expression of the dispersion relation, as derived for the meridionally unbounded case in § 5.3, cannot be derived for the meridionally bounded case because its eigenfunctions, unlike the Hermite functions of the meridionally unbounded case, do not satisfy (C 5) and (C 6).

To solve the equatorial balanced model for the meridionally bounded case, boundary conditions must be specified for the perturbation from the zonal mean flow. For the zonal mean flow itself no boundary conditions need to be specified because we have (5.10) and (5.11), which allows either $\bar{u}_R$ or $\bar{\eta}_R$ to be arbitrary. For the perturbation from the zonal mean flow, boundary conditions must be specified to solve two balance relations (5.17) and (5.18) with $D$ generalized to $D_\alpha$ in (5.43). It proves useful to rewrite them in the form

$$D_\alpha\left(\nabla \cdot \boldsymbol{u}_R'\right) = 3\frac{\beta^2}{c^2}yv_R', \tag{7.1}$$

$$D_\alpha\left(\beta y v_R' - c\frac{\partial \eta_R'}{\partial x}\right) = 3\beta\frac{\partial v_R'}{\partial y}. \tag{7.2}$$

Both are elliptic equations and therefore suitable boundary conditions must be specified for the terms in the brackets at the zonal boundaries. It is remarkable that balance relations (6.6) and (6.9), which are valid sufficiently far away from the equator, are identical to the terms in brackets set to zero. This suggests to place the zonal boundaries sufficiently far away from the equator so that zero Dirichlet boundary conditions can be used for the terms in brackets. Together with the boundary condition $v_R' = 0$, these imply that at the zonal boundaries $\partial\eta_R'/\partial x = 0$ and that $u_R'$ remains to be specified. Solving (7.1) and (7.2), which must be done iteratively because $v_R'$

is also unknown, gives $v'_R$, $\nabla \cdot \boldsymbol{u}'_R$ and $\eta'_R$. Since $q$ in (5.36) is given, we can thus also determine $\zeta'_R$. To obtain the velocity, we express it as $\boldsymbol{u}'_R = \hat{\boldsymbol{k}} \times \nabla\psi' + \nabla\chi'$, where $\psi'$ is the streamfunction and $\chi'$ the velocity potential. This gives the two Poisson equations $\nabla^2\psi' = \zeta'_R$ and $\nabla^2\chi' = \nabla \cdot \boldsymbol{u}'_R$, which can be solved by specifying at the zonal boundaries $v'_R$, which is zero, and $u'_R$ (Chen & Kuo 1992*a*, *b*). The boundary condition for $u'_R$ can initially be arbitrary, but then must evolve according to $\mathrm{D}u'_R/\mathrm{D}t = 0$ to guarantee the conservation of circulation. An equivalent condition also applies to the quasi-geostrophic model. It is derived by Phillips (1954) and is stated for example by (24) in McWilliams (1977). The equivalence becomes apparent by assuming that $u'_R$ is geostrophic, as it is the case for the quasi-geostrophic model, expressing it in terms of a streamfunction as $u'_R = \hat{\boldsymbol{k}} \times \nabla\psi'$, and integrating $\mathrm{D}u'_R/\mathrm{D}t = 0$ along the zonal boundaries.

Solid meridional boundaries in the zonal direction and in fact any arbitrarily shaped boundary are treated similarly, but pose the challenge of specifying appropriate boundary conditions for the terms in brackets in (7.1) and (7.2) at such boundaries.

### 7.2. *Forcing*

Forcing is incorporated by adding a mechanical force $\boldsymbol{F}_m$, such as wind forcing, to the right-hand side of (3.1) and a thermal force $F_t$, such as radiative relaxation, to the right-hand side of (3.2). Treating $\boldsymbol{F}_m$ and $F_t$ in the same way as the nonlinear terms in the same equations throughout the derivation of the equatorial balanced model results in (5.35) with the term $(\nabla \times \boldsymbol{F}_m - qF_t)/(c + \eta_R)$ added to the right-hand side.

### 7.3. *Stratification*

The simplest approach to extend the equatorial balanced model to describe stratified flows is to consider a stack of immiscible shallow layers of fluid with constant density, where the constant density in a layer is larger than that in the layer above it. The dynamics in each layer is described by the shallow water equations (3.1) and (3.2), except that $gh$ in (3.1) is replaced by the pressure in each layer, denoted by $p$, and that $h$ denotes the layer thickness. Each layer's thickness $h$ depends on the dynamical pressure in the same layer and on those in the layers above and below it (e.g. Mohebalhoje & Dritschel 2004), where the dynamical pressure in a layer is the pressure with its vertical variation within this layer omitted. This dependence dynamically couples the layers. The linear dynamics, however, can be decoupled by expanding $(\boldsymbol{u}, p, h)$ in terms of mutually orthogonal vertical modes (e.g. McWilliams 2006, § 5.1.3). This results in a set of evolution equations for the expansion coefficients of $(\boldsymbol{u}, p)$, whose linear form consists of closed sets of evolution equations for the coefficients of each vertical mode. Each of these sets is formally identical to the linear form of the shallow water equations of a single layer, given by (3.1) and (3.2). The vertical decomposition therefore allows to repeat the derivation of the equatorial balanced model for the case of a single layer by complete analogy for the case of a stack of layers.

For the case of continuous stratification the same general method can be applied to the Boussinesq equations as well as their hydrostatic approximation, that is, the primitive equations. In this case, too, the linear dynamics, decoupled through the use of vertical modes, is given by closed sets of evolution equations for the coefficients of each vertical mode, which is formally identical to the above case of a stack of layers.

## 8. Comparison with other balanced models

The most closely related balanced models to the equatorial balanced model introduced in this paper are those derived from the shallow water equations (3.3) and (3.4) rewritten in terms of the variables

$$q = \frac{\zeta + \beta y}{c + \eta}, \tag{8.1}$$

$$\delta = \nabla \cdot \boldsymbol{u}, \tag{8.2}$$

$$\gamma = f\zeta - c\nabla^2\eta - \beta u. \tag{8.3}$$

The resulting equations

$$\frac{\partial q}{\partial t} = \{-\boldsymbol{u} \cdot \nabla q\}, \tag{8.4}$$

$$\frac{\partial \delta}{\partial t} = \gamma + \{-\boldsymbol{u} \cdot \delta - \delta^2 + 2J(u, v)\}, \tag{8.5}$$

$$\begin{aligned}\frac{\partial \gamma}{\partial t} &= c^2\nabla^2\delta - f^2\delta - 2\beta f v + c\beta\frac{\partial \eta}{\partial x} \\ &\quad + \left\{-\boldsymbol{u} \cdot \nabla\gamma - \delta\gamma - \beta\delta u + \beta v\zeta + c\nabla\eta \cdot \nabla^2\boldsymbol{u} + c\eta\nabla^2\delta\right\}\end{aligned} \tag{8.6}$$

express the shallow water equations in $(q, \delta, \gamma)$-representation. The curly brackets are nonlinear terms.

The $(q, \delta, \gamma)$-representation allows for simple definitions of balance relations. This is best illustrated by the case of an $f$-plane, i.e. $f = f_0$ and $\beta = 0$, following by analogy the derivation of the quasi-geostrophic model on an $f$-plane in § 4. Fourier transforming the linearized form of (8.4)–(8.6) using (3.7) and (4.1) with $(\boldsymbol{u}, \eta)$ replaced by $(q, \delta, \gamma)$, allows to determine the eigenvectors spanning the phase space. Because of the change in variables the eigenvectors are not given by (4.5), but simply by $(\hat{\boldsymbol{e}}_R, \hat{\boldsymbol{e}}_{G^+}, \hat{\boldsymbol{e}}_{G^-}) = [(1\ 0\ 0), (0\ 1\ 0), (0\ 0\ 1)]$. The Rossby normal mode is thus represented purely by $q$ and the two gravity normal modes purely by $\delta$ and $\gamma$. The vector analogous to the vector in (4.8) is thus $\boldsymbol{e}_R = (1\ 0\ 0)$. Following the derivation below (4.8) by analogy, the two balance relations are therefore given by $\delta = \gamma = 0$. They are the geostrophic balance relation and therefore, when rewritten, give (4.10). The analogous steps from (4.12) to (4.14) can be carried out entirely in physical space, as explained in the second paragraph below (4.17). In this case this means substituting the geostrophic balance relation as given by (4.7) into (8.4)–(8.6) and multiplying the result from the left by $\boldsymbol{e}_R = (1\ 0\ 0)$, which trivially gives (4.14), except that $q$ is not given in its linear form (4.15) but its nonlinear form (8.1) in terms of (4.7). We thus have obtained a balanced model consisting of the evolution equation (8.4) and the two balance relations $\delta = \gamma = 0$. It represents a generalization of the quasi-geostrophic model on an $f$-plane.

For an equatorial $\beta$-plane, the analogous balanced model is not derived but defined to consist of evolution equation (8.4) and two balance relations given by $\delta = \gamma = 0$. Because $\delta = 0$ we can write $u = -\partial\psi/\partial y$ and $v = \partial\psi/\partial x$, $\psi$ being a streamfunction, and thus the balanced model in its linear form becomes

$$\frac{\partial}{\partial t}\left(\nabla^2\psi - \frac{\beta}{c}y\eta\right) = -\beta\frac{\partial \psi}{\partial x}, \tag{8.7}$$

$$\beta y\nabla^2\psi + \beta\frac{\partial \psi}{\partial y} - c\nabla^2\eta = 0. \tag{8.8}$$

This is strikingly similar to the linear form of the equatorial balanced model when (6.6) is valid, whereby the only difference is between one of their respective balance

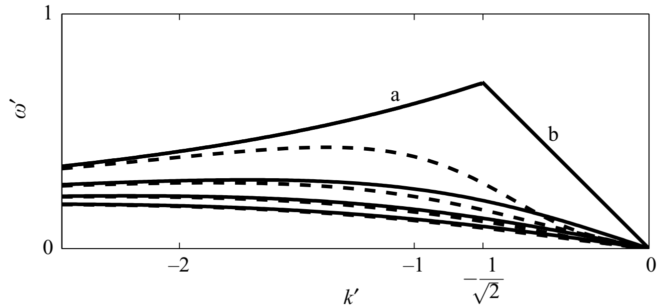


FIGURE 6. The common dispersion relation of the two balanced models with $\delta = \gamma = 0$ and $\delta = \delta^{(1)} = 0$ discussed in § 8. The solid curves are identical to those in figure 1 and are displayed for comparison.

relations, namely between (6.7) and (8.8). To determine the corresponding dispersion relation, we substitute $[\psi(\boldsymbol{x}, t), \eta(\boldsymbol{x}, t)] = [\hat{\psi}(y), \hat{\eta}(y)] \exp(\mathrm{i}kx - \mathrm{i}\omega t)$ into (8.7) and (8.8), non-dimensionalize using (6.1), expand $[\hat{\psi}(y), \hat{\eta}(y)]$ as a series in terms of Hermite functions similarly to (5.1), use (C 5), (C 6) and (C 8), eliminate $\hat{\eta}$, multiply by $\phi_m$, use (C 3), and truncate the series. This solution procedure leads to a generalized eigenvalue problem with eigenvalues of the form $k'/\omega'_R$, which can be solved numerically. The resulting dispersion relation is depicted by the dashed curves in figure 6. They should be compared with the dashed curves in figure 5, depicting the dispersion relation of the equatorial balanced model when (6.6) is valid. Despite the striking similarity mentioned above, a noticeably higher accurate representation of the dispersion relation of the shallow water equations, depicted by the solid curves in both figures, is achieved by the dispersion relation of the equatorial balanced model with approximation (6.6) than by that of the balanced model based on the two balance relations $\gamma = \delta = 0$.

Another comparison between the equatorial balanced model and the balanced model based on the two balance relations $\gamma = \delta = 0$ can be made sufficiently far away from the equator, where for the equatorial balanced model not only (6.6), but also (6.9) is valid. For this case, substituting (5.22) into (6.9) results in $\beta y \psi = c\eta$, where for clarity the subscript '$R$' and the primes have been dropped. Taking $\nabla^2$ gives $\gamma_2 = 0$, where

$$\gamma_2 = f\zeta - c\nabla^2\eta - 2\beta u, \tag{8.9}$$

with $f = \beta y$. Compared to $\gamma$ in (8.3) the only difference is the factor 2 in the last term. Replacing the one balance relation $\gamma = 0$ by $\gamma_2 = 0$ therefore changes the balance in such a way that the resulting balanced model becomes identical to the equatorial balanced model when (6.6) and (6.9) are valid and thus also to the modified quasi-geostrophic model introduced by Salmon (1982), described in § 6.1.

In its linearized form, the balanced model based on the two balance relations $\delta = \gamma = 0$, and therefore its dispersion relation shown in figure 6 (dashed curves), remains the same if its two balance relations were replaced by $\delta = \partial\delta/\partial t = 0$. These conditions were first suggested by Bolin (1955) and Charney (1955). They inspire an entire hierarchy of balanced models consisting of evolution equation (8.1) and the two balance relations $\delta^{(n)} = \delta^{(n+1)} = 0$, where $\delta^{(n)} = \partial^n\delta/\partial t^n$ and $\delta^{(0)} = \delta$ (Hinkelmann 1969; McIntyre & Norton 2000; Mohebalhojeh & Dritschel 2001). Similarly, another hierarchy is defined by using $\delta^{(n)} = \gamma^{(n)} = 0$ (Machenhauer 1977; Lorenz 1980; Tribbia 1984; Vautard & Legras 1986; Warn & Menard 1986; Mohebalhojeh & Dritschel 2001) and a third by $\gamma^{(n)} = \gamma^{(n+1)} = 0$ (Mohebalhojeh & Dritschel 2001). All models

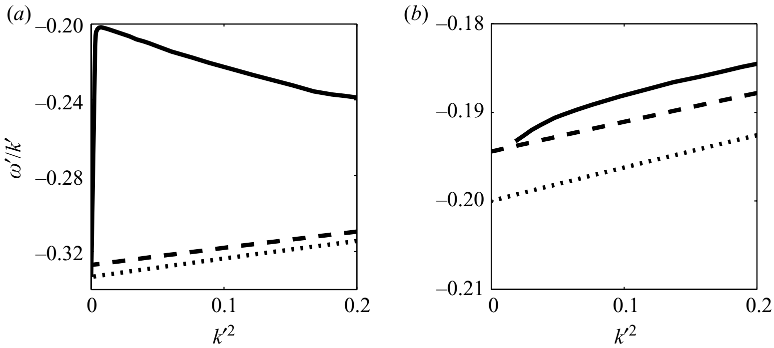


FIGURE 7. Comparison between the Bolin–Charney (solid curves), the equatorial balanced model (dashed curves) and the shallow water equations (dotted curves). Shown is $\omega'/k'$ as a function of $k'^2$, where the primes denote the non-dimensional variables in (6.1), for the cases (*a*) $n=1$ and (*b*) $n=2$. The solid curves are taken from figures 7 and 5 of Gent & McWilliams (1983), respectively. These curves exhibit singularities as $k'^2$ tends to zero, which Gent & McWilliams (1983) refer to as (*a*) "discontinuous" and (*b*) "infinite slope".

with $n>0$ do not share the simplicity of the equatorial balanced model and we do not compare them with it.

The Bolin–Charney model (Bolin 1955; Charney 1955, 1962), or balance equations, is another balanced model also valid in the equatorial region. It consists of the evolution equation (8.1) and two balance relations. One is obtained by applying $\delta=\partial\delta/\partial t=0$ to (8.5), resulting in what is known as the Bolin–Charney balance equation

$$\gamma_\psi + 2J(u_\psi, v_\psi) = 0, \tag{8.10}$$

where $\gamma_\psi$ is given by $\gamma$ in (8.3) with $u$ in the last term replaced by $u_\psi$. The subscript $\psi$ denotes the rotational velocity component, whereas the velocity is not necessarily purely rotational. The other balance relation is obtained by taking the time derivative of (8.10), resulting in an expression given in terms of the time derivatives of $\zeta$ and $\eta$. The time derivatives are then replaced using shallow water equations (3.3) and (3.4), where the velocity is not purely rotational. The Bolin–Charney model thus describes divergent flow. In their linearized forms, the Bolin-Charney model and the balanced model based on the two balance relations $\gamma=\gamma^{(1)}=0$ are identical. A detailed discussion of the Bolin–Charney model and its generalization to arbitrarily high order is given by Mohebalhoje & McIntyre (2007*a*).

The dispersion relation of the Bolin–Charney model is studied by Gent & McWilliams (1983), who in particular identify singularities in the small-wavenumber limit of $\omega/k$ as a function of $k^2$. Figure 7 shows their results (solid curves), where they refer to the singularity as $k^2$ tends to zero in (*a*) as 'discontinuous' and in (*b*) as 'infinite slope'. These singularities do not appear in the shallow water equations themselves (dotted curves) and the equatorial balanced model (dashed curves). When compared with the Bolin–Charney model, the figure also shows that the equatorial balanced model approximates $\omega/k$ of the shallow water equations more accurately. In the equatorial balanced model, this small-wavenumber limit can be improved even further by tuning the parameter $\alpha$. However, there may arise some adverse effects on other desirable aspects of the equatorial balanced model.

## 9. Conclusion

A balanced model on an equatorial $\beta$-plane, referred to as the equatorial balanced model, is derived from the shallow water equations. Its derivation is carried out within the general geometric framework used by Leith (1980) for his derivation of the quasi-geostrophic model on an $f$-plane. In this sense, the equatorial balanced model represents the equatorial counterpart of the quasi-geostrophic model. It consists of the evolution equation of potential vorticity (5.35) and has two balance relations, respectively, (5.10) and (5.11) for the zonal mean flow and (5.17) and (5.18), with the generalized modified Helmholtz operator $D_\alpha$ in (5.43) replacing the operator $D$, for the perturbation from the zonal mean flow. These balance relations describe the intricate balance of forces in the equatorial region in contrast to the simple balance of two dominant forces described by geostrophic balance outside the equatorial region. The equatorial balanced model's dispersion relation (5.44) approximates those of the equatorial Rossby waves and the Rossby-wave part of the mixed Rossby–gravity wave of the shallow water equations remarkably well, as seen in figure 3. An interesting feature is the presence of a free parameter $\alpha$, giving us the power to adjust the model for a specific purpose. To obtain the accurate dispersion relation, we set $\alpha = 2.5$. The equatorial balanced models can be extended to describe also bounded, forced, and stratified fluids. In comparison with balanced models of equal simplicity the equatorial balanced model is more accurate if the dispersion relation of equatorial waves is the prime concern. The lack of singularities of any kind like those noted by Gent & McWilliams (1983) for the Bolin–Charney model, or balance equations, should be noted in particular.

The two balance relations of the equatorial balanced model for perturbations from zonal mean flow (5.17) and (5.18) can be approximated under certain conditions. In the equatorial region and beyond, except for small wavenumbers for which the farthest possible distance from the equator decreases with decreasing wavenumber, the balance relation (5.17) can be approximated by (6.6). With this approximation, the dispersion relation (dashed curves in figure 5) remains remarkably accurate, except that of the Rossby-wave part of the mixed Rossby–gravity wave at small wavenumbers. Sufficiently far away from the equator, the other balance relation (5.18) can be approximated by geostrophy in the zonal direction, leading to $\lambda^2$ (6.9). When both approximations are valid the equatorial balanced model becomes identical to the modified quasi-geostophic model introduced by Salmon (1982). At and very near the equator, approximation (6.6) is also valid and approximation (6.9) is replaced by approximation (6.11).

This research was supported by the National Science Foundation under Grant No. OCE-0550658. ARM would like to thank the UK Natural Environment Research Council for a research fellowship and the Universities of St. Andrews and Tehran for the support during this research.

## Appendix A. Definition of conjugate transpose and Hermitian

The complex inner product of any two $N$-dimensional vector functions $\boldsymbol{a}(\boldsymbol{x})$ and $\boldsymbol{c}(\boldsymbol{x})$ is defined by

$$\langle \boldsymbol{a}(\boldsymbol{x}), \boldsymbol{c}(\boldsymbol{x}) \rangle = \int \sum_{n=1}^{N} a_n(\boldsymbol{x}) c_n^*(\boldsymbol{x})\, \mathrm{d}\boldsymbol{x}, \tag{A 1}$$

where '$*$' denotes the complex conjugate and the integral is over a specified space. Let us assume that $\boldsymbol{a}(\boldsymbol{x}) = \boldsymbol{O}(\boldsymbol{x})\boldsymbol{b}(\boldsymbol{x})$, where $\boldsymbol{O}(\boldsymbol{x})$ is a matrix operator and $\boldsymbol{b}(\boldsymbol{x})$ a vector function both with appropriate dimensions. For example, $\boldsymbol{O}(\boldsymbol{x})$ can be square, as $\mathscr{L}$ in (3.5), or a vector, as $\hat{\boldsymbol{e}}_R$ in (4.5), and thus $\boldsymbol{b}(\boldsymbol{x})$ must be $N$- and 1-dimensional, respectively. The conjugate transpose, or adjoint, of $\boldsymbol{O}(\boldsymbol{x})$, denoted by '†', is defined by

$$\langle \boldsymbol{O}(\boldsymbol{x})\boldsymbol{b}(\boldsymbol{x}), \boldsymbol{c}(\boldsymbol{x})\rangle = \langle \boldsymbol{b}(\boldsymbol{x}), \boldsymbol{O}^{\dagger}(\boldsymbol{x})\boldsymbol{c}(\boldsymbol{x})\rangle. \tag{A 2}$$

If $\boldsymbol{O}(\boldsymbol{x})$ is given in terms of differential operators, calculating its conjugate transpose involves integrations by parts. A Hermitian, or self-adjoint, $\boldsymbol{O}(\boldsymbol{x})$ is defined by $\boldsymbol{O}^{\dagger}(\boldsymbol{x}) = \boldsymbol{O}(\boldsymbol{x})$.

## Appendix B. Steps from (3.8) to (3.9)

We first interchange the rows of the matrix in (3.8), whereby the first becomes the second, the second becomes the third, and the third becomes the first. We then calculate consecutively, new 3rd row $= \omega \cdot$ 3rd row $-\, \mathrm{i}f \cdot$ 2nd row, new 2nd row $= ck \cdot$ 2nd row $+\, \omega \cdot$ 1st row, new 1st row $= (\omega^2 - c^2k^2)/(ck) \cdot$ 1st row $-\, \omega/(ck) \cdot$ 2nd row, new 3rd row $= (c^2k^2 - \omega^2) \cdot$ 3rd row $+\, (\mathrm{i}c\omega\partial/\partial y + \mathrm{i}cfk) \cdot$ 2nd row, $1/c^2 \cdot$ 1st row, $-1/c^2 \cdot$ 2nd row and $1/(c^2\omega) \cdot$ 3rd row, which gives (3.9).

## Appendix C. Hermite functions

The Hermite functions are defined by

$$\phi_n(y') = \frac{1}{\sqrt{n!2^n\sqrt{\pi}}}\mathrm{e}^{-y'^2/2}H_n(y'), \tag{C 1}$$

where $y'$ is non-dimensional to be distinguished from the dimensional $y = \sqrt{c/\beta}\,y'$ used throughout the paper, $n = 0, 1, 2, \ldots$ and $-\infty < y' < \infty$. The functions $H_n(y')$ are the Hermite polynomials (Abramowitz & Stegun 1964, Chapter 22), which can be obtained using the recurrence relation

$$H_{n+1}(y') = 2y'H_n(y') - 2nH_{n-1}(y') \tag{C 2}$$

with $H_0(y') = 1$. The Hermite functions form a complete set of orthonormal functions, expressed by

$$\int_{-\infty}^{\infty} \phi_n(y')\phi_m(y')\mathrm{d}y' = \delta_{nm}, \tag{C 3}$$

where $\delta_{nm}$ is the Kronecker delta. Using (C 2) and the fact that the Hermite polynomials satisfy the differential equation

$$\frac{\mathrm{d}H_n(y')}{\mathrm{d}y'} = 2nH_{n-1}(y'), \tag{C 4}$$

allows to derive

$$y'\phi_n = \frac{1}{\sqrt{2}}(\sqrt{n}\phi_{n-1} + \sqrt{n+1}\phi_{n+1}), \tag{C 5}$$

$$\frac{\mathrm{d}\phi_n}{\mathrm{d}y'} = \frac{1}{\sqrt{2}}(\sqrt{n}\phi_{n-1} - \sqrt{n+1}\phi_{n+1}). \tag{C 6}$$

Substituting (C 5) and (C 6) into the identity

$$\left(\frac{\mathrm{d}}{\mathrm{d}y'} + y'\right)\left(\frac{\mathrm{d}}{\mathrm{d}y'} - y'\right)\phi_n = \left(\frac{\mathrm{d}^2}{\mathrm{d}y'^2} - 1 - y'^2\right)\phi_n, \tag{C 7}$$

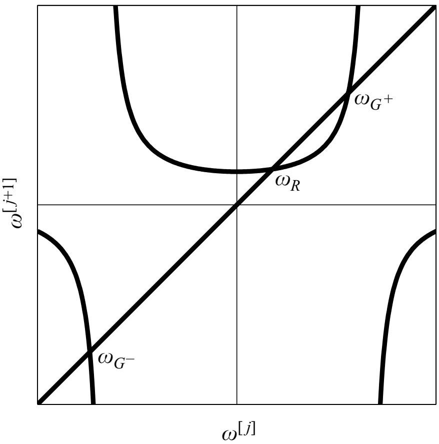


FIGURE 8. Iteration: the function $\omega^{[j+1]}(\omega^{[j]})$ in (5.8) and the diagonal line $\omega^{[j+1]} = \omega^{[j]}$ is depicted.

gives

$$\frac{\mathrm{d}^2\phi_n}{\mathrm{d}y'^2} = -(2n+1-y'^2)\phi_n. \tag{C 8}$$

In terms of the dimensional coordinate $y$ defined above, this becomes

$$-(1+2n)\,\frac{\beta}{c}\phi_n = \left(\frac{\mathrm{d}^2}{\mathrm{d}y'^2} - \frac{\beta^2}{c^2}y^2\right)\phi_n, \tag{C 9}$$

which can be generalized to $\hat{D}\phi_n = D\phi_n$ with $\hat{D}$ and $D$ given by (5.16) and (5.19), respectively. Multiplication by $\hat{D}^{-1}D^{-1}$ results in

$$D^{-1}\phi_n = \hat{D}^{-1}\phi_n. \tag{C 10}$$

## Appendix D. Iteration

Figure 8 shows the general shape of the function $\omega^{[j+1]}(\omega^{[j]})$ in (5.8) for each $k<0$ and $n \geqslant 0$. The three points where it intersects the diagonal line, which indicates $\omega^{[j+1]} = \omega^{[j]}$, represent the three solutions of (5.6). For $k = -\sqrt{\beta/c}/\sqrt{2}$ and $n=0$, the two intersections at $\omega_R$ and $\omega_{G^+}$ coincide. The figure shows that by choosing $\omega^{[0]}=0$ as the first guess, the iteration in (5.8) results in the convergence of $\omega^{[j]}$ to $\omega_R$ as $j$ increases.

REFERENCES


ABRAMOWITZ, M. & STEGUN, I. 1964, *Handbook of Mathematical Functions with Formulas, Graphs, and Mathematical Tables*. Dover.

BAER, F. 1977 Adjustment of initial conditions required to suppress gravity oscillations in nonlinear initialization. *Beitr. Phys. Atmos.* **50**, 350–366.

BAER, F. & TRIBBIA, J. 1977 On complete filtering of gravity modes through nonlinear initialization. *Mon. Wea. Rev.* **105**, 1536–1539.

BOKHOVE, O. 1997 Slaving principles, balanced dynamics, and the hydrostatic Boussinesq equations. *J. Atmos. Sci.* **54**, 1662–1674.

BOLIN, B. 1955 Numerical forecasting with the barotropic model. *Tellus* **7**, 27–49.

CANE, M. & SARACHIK, E. 1979 Forced baroclinic ocean motions, III: the linear equatorial basin case. *J. Mar. Res.* **37**, 355–398.

CHARNEY, J. 1955 The use of the primitive equations of motion in numerical forecasting. *Tellus* **7**, 22–26.

Charney, J. 1962 Integration of the primitive and balance equations. *Proceedings of the International Symposium on Numerical Weather Prediction* (ed. S. Syôno), pp. 131–152. Meteorological Society of Japan, Tokyo, Japan.

Chen, Q. & Kuo, Y. 1992*a* A harmonic-sine series expansion and its application to partitioning and reconstruction problems in a limited area. *Mon. Wea. Rev.* **120**, 91–112.

Chen, Q. & Kuo, Y. 1992*b* A consistency condition for wind-field reconstruction in a limited area and a harmonic-cosine series expansion. *Mon. Wea. Rev.* **120**, 2653–2670.

Ford, R., McIntyre, M. & Norton, W. 2000 Balance and the slow quasimanifold: some explicit results. *J. Atmos. Sci.* **57**, 1236–1254.

Gent, P. & McWilliams, J. 1983 The equatorial waves of balanced models. *J. Phys. Ocean.* **13**, 1179–1192.

Gill, A. 1982 *Atmosphere-Ocean Dynamics*, 662 pp. Academic Press.

Groove, L. 2004 *Algebra*, 320 pp. Dover Publications.

Hinkelmann, K. 1969 Primitive equations. *Lectures in Numerical Short-Range Weather Prediction*, Moscow, WMO No. 297, 306–375.

Leith, C. 1980 Nonlinear normal mode initialization and quasi-geostrophic theory. *J. Atmos. Sci.* **37**, 958–968.

Lorenz, E. 1980 Attractor sets and quasi-geostrophic equilibrium. *J. Atmos. Sci.* **37**, 1685–1699.

Machenhauer, B. 1977 On the dynamics of gravity oscillations in a shallow water model, with application to normal mode initialization. *Beitr. Phys. Atmos.* **50**, 253–271.

Matsuno, T. 1966 Quasi-geostrophic motions in the equatorial area. *J. Meteorol. Soc. Jpn.* **44**, 25–42.

McIntyre, M. & Norton, W. 2000 Potential vorticity inversion on a hemisphere. *J. Atmos. Sci.* **57**, 1214–1235.

McWilliams, J. 1977 A note on a consistent quasi-geostrophic model in a multiply connected domain. *Dyn. Atmos. Oceans* **1**, 427–441.

McWilliams, J. 2006 *Fundamentals of Geophysical Fluid Dynamics*, 249 pp. Cambridge University Press.

Mohebalhoje, A. & Dritschel, D. 2004 Contour-advective semi-Lagrangian algorithms for many-layer primitive equation models. *Q. J. Roy. Met. Soc.* **130**, 347–364.

Mohebalhoje, A. & McIntyre, M. 2007*a* Local mass conservation and velocity splitting in PV-based balanced models. Part I. The hyperbalance equations. *J. Atmos. Sci.* **64**, 1782–1793.

Mohebalhoje, A. & McIntyre, M. 2007*b* Local mass conservation and velocity splitting in PV-based balanced models. Part II. Numerical results. *J. Atmos. Sci.* **64**, 1794–1810.

Mohebalhojeh, A. & Dritschel, D. 2001 Hierarchies of balance conditions for the $f$-plane shallow water equations. *J. Atmos. Sci.* **58**, 2411–2426.

Moore, D. & Philander, S. G. H. 1977 Modeling of the tropical oceanic circulation. In *Marine Modeling, The Sea*, pp. 319–361. John Wiley & Sons, Wiley Interscience.

Pedlosky, J. 1987 *Geophysical Fluid Dynamics*, 2nd edition, 710 pp. Springer Verlag.

Phillips, P. 1954 Energy transformations and meridonal circulations associated with simple baroclinic waves in a two-level, quasi-geostrophic model. *Tellus* **6**, 273–286.

Salmon, R. 1982 Geostrophic turbulence. In *Topics in Ocean Physics* (ed. A. Osborne and P. Rizzoli), 550 pp. Proceedings of the International School Enrico Fermi.

Salmon, R. 1998 *Lectures on Geophysical Fluid Dynamics*, 378 pp. Oxford University Press.

Theiss, J. 2004 Equatorward energy cascade, critical latitude, and the predominance of cyclonic vortices in geostrophic turbulence. *J. Phys. Ocean.* **34**, 1663–1678.

Tribbia, J. 1979 Nonlinear initialization on an equatorial beta-plane. *Mon. Wea. Rev.* **107**, 704–713.

Tribbia, J. 1984 A simple scheme for high-order nonlinear normal mode initialization. *Mon. Wea. Rev.* **112**, 278–284.

Vallis, G. K. 2006 *Atmospheric and Oceanic Fluid Dynamics: Fundamentals and Large-Scale Circulation*, 745 pp. Cambridge University Press.

Vautard, R. & Legras, B 1986 Invariant manifolds, quasi-geostrophy and initialization. *J. Atmos. Sci.* **43**, 565–584.

Warn, T. & Menard, R. 1986 Nonlinear balance and gravity-inertial wave saturation in a simple atmospheric model. *Tellus* **38**A, 285–294.

Wilkinson, J. 1988 *The Algebraic Eigenvalue Problem*. Oxford University Press.